Mobile Non-Invasive Weigh-in-Motion System

FDOT Contract 16507036

Submitted to

The Florida Department of Transportation

Research Center

605 Suwannee Street, MS 30

Tallahassee, FL 32399

Mr. Craig Wilson

Motor Carrier Compliance Office

Submitted by

Dr. Amr Oloufa (PI)

Dr. Faissal Moslehy (CO-PI)

College of Engineering and Computer Science

University of Central Florida

4000 Central Florida Blvd.

Orland, FL 32816

Final Report

November 2008

Disclaimer

The opinions, findings, and conclusions expressed in this publication are those of the authors and not necessarily those of the State of Florida Department of Transportation.

Metric Conversion

APPROXIMATE CONVERSIONS TO SI UNITS

SYMBOL	WHEN YOU KNOW	MULTIPLY BY	TO FIND	SYMBOL
LENGTH				
in	inches	25.4	millimeters	mm
ft	feet	0.305	meters	m
yd	yards	0.914	meters	m
mi	miles	1.61	kilometers	km
SYMBOL	WHEN YOU KNOW	MULTIPLY BY	TO FIND	SYMBOL
AREA				
in2	square inches	645.2	square millimeters	mm2
ft2	square feet	0.093	square meters	m2
yd2	square yard	0.836	square meters	m2
ac	acres	0.405	hectares	ha
mi2	square miles	2.59	square kilometers	km2
SYMBOL	WHEN YOU KNOW	MULTIPLY BY	TO FIND	SYMBOL
VOLUME				
fl oz	fluid ounces	29.57	milliliters	mL
gal	gallons	3.785	liters	L
ft3	cubic feet	0.028	cubic meters	m3
yd3	cubic yards	0.765	cubic meters	m3
SYMBOL	WHEN YOU KNOW	MULTIPLY BY	TO FIND	SYMBOL
MASS				
oz	ounces	28.35	grams	g
lb	pounds	0.454	kilograms	kg
T	short tons (2000 lb)	0.907	megagrams (or "metric ton")	Mg (or "t")
SYMBOL	WHEN YOU KNOW	MULTIPLY BY	TO FIND	SYMBOL
TEMPERATURE (exact degrees)				
^{o}F	Fahrenheit	5 (F-32)/9 or (F-32)/1.8	Celsius	^{o}C
SYMBOL	WHEN YOU KNOW	MULTIPLY BY	TO FIND	SYMBOL
ILLUMINATION				
fc	foot-candles	10.76	lux	lx
fl	foot-Lamberts	3.426	candela/m2	cd/m2
SYMBOL	WHEN YOU KNOW	MULTIPLY BY	TO FIND	SYMBOL
FORCE and PRESSURE or STRESS				
lbf	poundforce	4.45	newtons	N
lbf/in2	poundforce per square inch	6.89	kilopascals	kPa

Adapted from Federal Highway Administration, "SI* (MODERN METRIC) CONVERSION FACTORS" found at http://www.fhwa.dot.gov/aaa/metricp.htm, accessed on July 5, 2008.

Technical Report Documentation Page

1. Report No.	2. Government Accession No.	3. Recipient's Catalog No.
4. Title and Subtitle Mobile Non-Invasive Weigh-in-Motion System		5. Report Date November 2008
		6. Performing Organization Code
7. Author(s) Amr A. Oloufa, P.E. Faissal M. Moslehy, P.E.		8. Performing Organization Report No.
9. Performing Organization Name and Address Center for Advanced Transportation Systems Simulation University of Central Florida P.O. Box 162450, Orlando, FL 32816-2450		10. Work Unit No. (TRAIS)
		11. Contract or Grant No. 16507036
12. Sponsoring Agency Name and Address Florida Department of Transportation 605 Suwannee Street, MS 30 Tallahassee, FL 32399		13. Type of Report and Period Covered Final Report
		14. Sponsoring Agency Code FDOT

15. Supplementary Notes

16. Abstract

Existing weigh-in-motion (WIM) technologies weigh heavy vehicles at highway speeds. However, the high cost and fixed location of existing WIM systems limit the number of systems that can be installed and make it possible for them to be avoided by overweight vehicles. Low-cost portable WIM systems could allow governments to install more systems and vary the location of such systems, thus reducing the possibility that overweight vehicles will be able to avoid enforcement.

This paper reports on a series of six experiments performed to develop a low-cost system for weighing heavy vehicles at highway speed. The system consists of a metal strip instrumented with acoustic emission sensors that detect acoustic waves within the metal material when a vehicle drives over the metal strip.

Correlations were found between the weight of the vehicle crossing the metal strip and the acoustic response recorded by the computer. Unfortunately, the variability of the acoustic emission response was fairly high, resulting in imprecise values for predicted vehicle weight. Future research should consider ways to reduce the variability of the acoustic emission response. An improved version of the WIM system created for this project could be beneficial in a range of areas including weight enforcement, planning, and safety.

17. Key Word	18. Distribution Statement
weigh-in-motion	No restriction. This document is available to the public.

19. Security Classif. (of this report)	20. Security Classif. (of this page)	21. No. of Pages	22. Price
Unclassified	Unclassified	57	

Executive Summary

Almost everything consumed is carried by trucks at some point in the journey regardless of the principal mode, whether it is by rail, ship, water, or plane. Trucks carry a large share of freight compared to the other modes: 70 percent of total value, 60 percent of total weight, and 34 percent of ton-miles. From 1980 to 2002, truck travel grew by 90 percent. Freight volumes are expected to continue to increase rapidly through 2020. (U.S. Department of Transportation, 2006)

The expected increase in the number of trucks on our highways, coupled with modern logistic practices and the rapid growth in e-commerce may change traffic flow characteristics on highways significantly. This will require the application of new and innovative technologies to expedite the monitoring of commercial vehicle conformance to regulations governing weight, dimensions, and safety, as mandated by the Department of Transportation.

A number of weigh-in-motion (WIM) technologies have been developed to facilitate the weighing of heavy vehicles at highway speeds, eliminating the need to stop compliant vehicles and reducing delay due to weighing procedures. However, the high cost of a WIM system limits the number of systems that can be installed. Additionally, because they must be placed in the pavement and therefore must have a fixed location, they can be avoided by overweight vehicles. Low-cost portable WIM systems could be used to expand the influence of weight enforcement by allowing governments to install more systems. Additionally, the portability of such a system would allow agencies to vary the location, thus reducing the possibility that overweight vehicles will be able to avoid enforcement.

This paper reports on a series of six experiments performed as part of FDOT Contract 16507036 to develop a low-cost system for weighing heavy vehicles at highway speed. The system consists of a metal strip instrumented with acoustic emission sensors to detect acoustic waves within the metal material. When a vehicle drives over the metal strip, acoustic waves are created within the metal strip, transmitted to a computer via the acoustic emission sensors, and measured using a software program.

The development of a low-cost WIM system involved several steps, including:

- purchasing the appropriate equipment,
- determining the relationship between the weight of a vehicle crossing the metal strip and the acoustic emission response,
- searching for other parameters that could help to predict the weight of the vehicle based on the acoustic emission response,
- examining the variability of the predicted weights, and
- evaluating the efficacy and constructability of the system.

The researchers were able to find correlations between the weight of the vehicle crossing the metal strip and the acoustic response recorded by the computer. The energy and absolute energy of the acoustic emission response were found to be particularly important for predicting the

vehicle weight. In addition, the speed of the vehicle and the location along the metal strip where the vehicle's tires strike the strip are helpful in the prediction of the vehicle weight.

The variability of the acoustic emission response was fairly high, resulting in imprecise values for predicted vehicle weight. Future research to examine this technology further should consider ways to reduce the variability of the acoustic emission response, including by improving the software and hardware used by the sensors and by machining a more uniform test strip.

An improved version of the WIM system created for this project could be beneficial in a range of areas. Among others, such systems could be used to:

- increase the number of weight enforcement sites throughout the state,
- target areas where non-compliant vehicles are suspected of regularly using the roadway,
- improve pavement design by providing a more accurate representation of the weights of vehicles using specific roadways, or
- improve safety by warning overweight vehicles at restricted bridge crossings.

Table of Contents

Table of Contents (continued)

List of Figures

List of Tables

1 Introduction

Almost everything consumed is carried by trucks at some point in the journey regardless of the principal mode of transport, whether it is by rail, ship, water, or plane. Trucks carry a large share of freight compared to the other modes: 70 percent of total value, 60 percent of total weight, and 34 percent of ton-miles. From 1980 to 2002, truck travel grew by 90 percent. Freight volumes are expected to continue to increase rapidly through 2020. (U.S. Department of Transportation, 2006)

The expected increase in the number of trucks on our highways, coupled with modern logistic practices and the rapid growth in e-commerce may change traffic flow characteristics on highways significantly. This will require the application of new and innovative technologies to expedite the monitoring of commercial vehicle conformance to regulations governing weight, dimensions, and safety, as mandated by the Department of Transportation.

1.1 Background

It has long been known that some commercial vehicle operators that exceed safe weight limits for their vehicles often bypass fixed weigh stations. (Cunagin, Mickler, & Wright, 1997) Since it is documented that the pavement deterioration that is attributable to overweight vehicles is considerable, (Barros, 1985) the development of mobile stations (or virtual weigh stations) that can detect attempts to bypass weigh stations is an extremely valuable goal.

Generally, existing weigh-in-motion (WIM) systems require embedding relatively large sensors into the road surface. This process also requires special preparation of the roadway approach surface just prior to and immediately after the embedded sensor to eliminate potential extraneous dynamic effects produced by the wheel impact on the sensor due to unevenness of the roadway. (Izadmehr & Lee, 1987) Since one of the major benefits of virtual weigh stations is the ability to move them around, having a large embedded WIM sensor is clearly undesirable for this application.

In other areas, several industries have been developing technologies that enable estimation of operational parameters using non-destructive evaluation for detection of anomalies, assessment of fluid flow, and measurement of stresses by correlating information from a variety of sensors. These technologies include laser speckle interferometry, shearography, and velocimetry, as well as acoustic and ultrasonic sensors. Recognizing that these technologies might be used to create a low-cost WIM sensor, the researchers proposed to the Center for Advanced Transportation Systems Simulation at University of Central Florida (UCF) that a pilot study of some of these sensors be implemented. The study was completed in 2003. Because it showed promise for the development of a low-cost WIM system, the concept was studied further, as presented in this report.

1.2 Experimental Concept

When a vehicle rolls over an object, it sets up a vibration within the object. It is possible to detect the acoustic emissions of the vibration using acoustic emission sensors. These vibrations are affected by the speed of the vehicle, the weight of the vehicle, and the distance of the tires from

the acoustic emission sensors. Determining the weight of the vehicle then becomes an inverse problem of the equation shown below in which the output (the acoustic emission signal) is known and the input (the weight of the vehicle) is unknown.

$$u(t) = \int_0^t G(t-\tau)P(\tau)d\tau$$

The proposed WIM system consists of a metal strip that is laid across the roadway with acoustic emission sensors attached. The signal from the sensors is run through a preamplifier which sends the acoustic emission signal on to a computer where the signal is analyzed using acoustic emission software. To solve the inverse problem, an experiment must be run using a test vehicle driving over the metal strip. The weight of the vehicle, the speed of the vehicle, and the horizontal location along the metal strip where the tires strike the test strip is known, but varied. Statistical analysis performed on the output of this experiment (the acoustic emission signal), given the input variables (weight, speed, and tire location), establish the correlation between the acoustic emission signal and the weight of the vehicle.

1.3 Objectives

This project involved the development and testing of an extremely low-cost WIM system comprising acoustic technologies integrated with a low profile metal strip that is glued to the roadway surface. It involved instrumenting a metal strip with an acoustic sensor as shown in Figure 1. Two strip types (architectures) were to be evaluated. The first type, referred to as configuration A, was a simple strip with acoustic sensors attached to the surface, as shown in Figure 2. The second type, referred to as configuration B, consisted of two strips with one acoustic sensor embedded in each strip, as shown in Figure 3, and allowed the user to find the load per wheel, not just per axle. A diagram of the cross section of configuration B is shown in Figure 4.

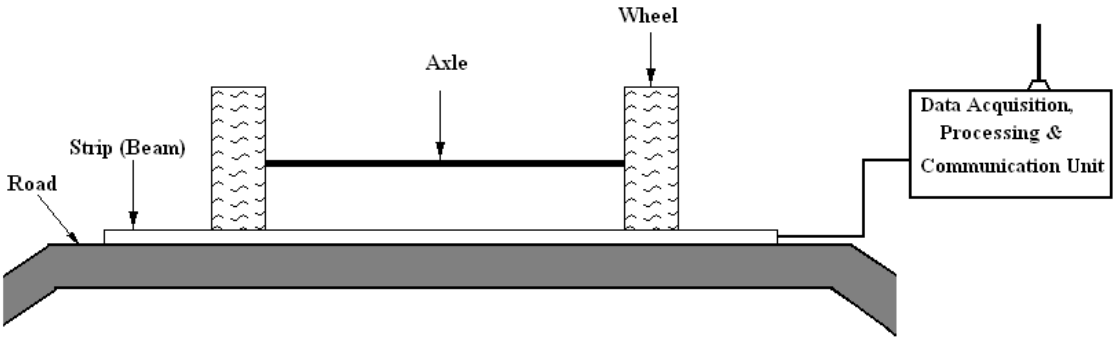

Figure 1 Basic architecture of acoustic sensor system

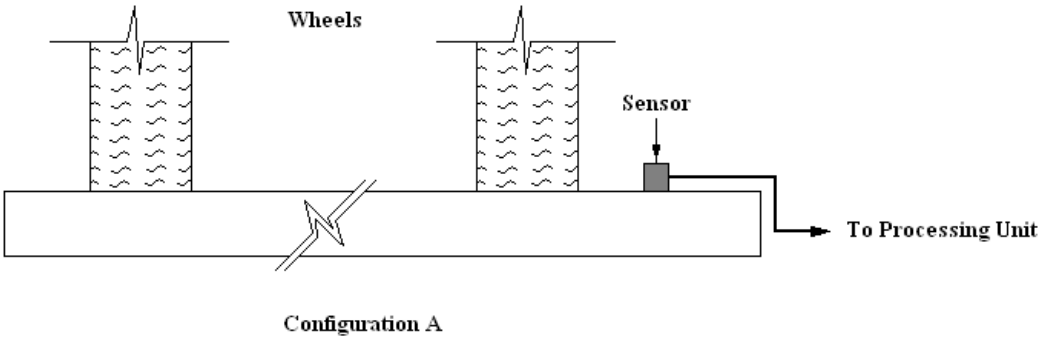

Figure 2 Architecture for configuration A

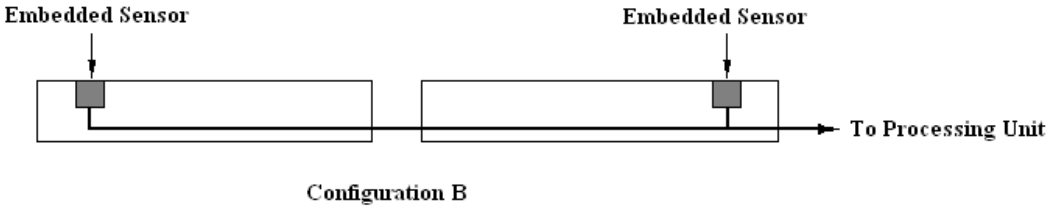

Figure 3 Architecture for configuration B

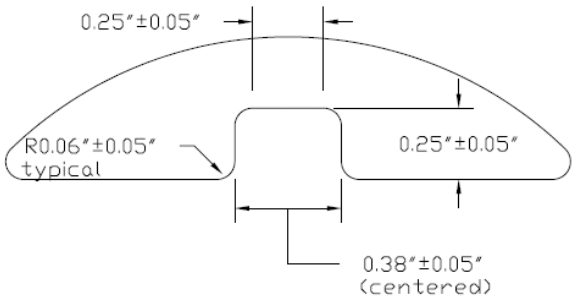

Figure 4 Cross section for configuration B

2 Literature Review

In an effort to extend the useful life of roadway pavement and improve vehicle safety, weight limits have been set for heavy trucks utilizing the nation's highways. (*Truck Weight Limits: Issues and Options, Special Report 225*, 1990) To enforce the weight limits, trucks are weighed at weigh stations along the highway and overweight vehicles are ticketed and/or fined. Weigh stations take a variety of forms, including:

- traditional weigh stations where heavy vehicles are pulled off of the highway and weighed on low-speed WIM scales and/or stationary scales, and
- Remotely Operated Compliance Stations (ROCS™) where heavy vehicles are weighed at highway speeds in the travel lanes. (Chang, Sverdlova, Sonmez, & Strit, 2000; Collap, Al Hakim, & Thom, 2002; Moslehy & Oloufa, 2004; Papagiannakis, 1997; Stergioulas, Cebon, & Macleod, 2000)

Typical weigh stations collect information about axle weight, axle configuration and spacing, and whole vehicle weight. In addition to weight enforcement, this data can also be used for a variety of transportation planning purposes, including the design of pavement and bridge structures, planning transportation facilities, and safety analysis. (Hajek, Kennepohl, & Billing, 1992)

Static scales measure the weight of a vehicle at rest. Because of the large size of the vehicles involved, the scales are usually built to weigh only one axle at a time. That is, the vehicle is parked with just the front axles on the scale and the weight is measured, then the vehicle is moved so that the second set of axles rests on the scale, and so forth. Accurate measurement relies upon level pavement around the scale and upon the elimination of other sources of error such as load shifting between measurements. (Davies & Sommerville, 1987)

WIM systems, on the other hand, measure the dynamic forces associated with a vehicle in motion passing over the scale. The accuracy of a WIM system is affected by the type of suspension system present in the vehicle being weighed, the type of pavement (flexible or rigid), and the profile of the pavement surrounding the scale. (Cunagin, Majdi, & Yeom, 1991)

Several different technologies are currently in use in WIM systems. The bending plate WIM system consists of steel plates surrounded by rubber and connected to strain gauges. The vehicle weight is related to the strain on the plates as the vehicle crosses over them. (Sebaaly, Chizewick, Wass, & Cunagin, 1991) Similarly, a WIM system can be created by measuring strain in a structure (a bridge, for instance). (Gagarine, Flood, & Albrecht, 1992)

The hydraulic load cell WIM system consists of a steel platform that acts as the load bearing surface and transfers the load to a piston. (Sebaaly et al., 1991)

The piezoelectric WIM system works by measuring voltage differences that are caused by the pressure that is exerted on a sensor when the vehicle passes over it. (Andrle, McCall, & Kroeger, 2002)

All of the WIM systems described above are fixed systems, meaning that they are installed in the pavement in the traffic lane. A major drawback of fixed weigh stations is that their location

becomes generally known among truck drivers, making it possible for non-compliant vehicles to avoid detection by using an alternate route, such as traveling on local roads in the vicinity of the weigh station. In addition, the high cost of these scales makes it impractical to create a cordon by placing them on all possible routes in an area. (Cunagin et al., 1997)

To overcome some of the problems with fixed systems, portable systems have been developed. The capacitance mat is one such system. It consists of a three plate capacitor within a tuned circuit (made from three sheets of steel surrounded by rubber dielectric). A passing vehicle compresses the capacitor, changing the frequency of oscillation. This change in frequency can be related to the weight of the vehicle. (Cole & Cebon, 1989; Sebaaly et al., 1991)

Another portable WIM system that has been developed is a fiber optic system where the weight of the vehicle is measured by the bending of light. (Mimbela, Pate, Copeland, Kent, & Hamrick, 2003)

Other than papers produced as part of this project, no other citations were found that use acoustic emission technology for the purpose of weighing heavy vehicles in motion. A description of the laboratory test equipment and the results of Experiment C (see below) were first published in the Proceedings of the 2007 International Conference on Industry, Engineering, and Management Systems. (Moslehy, Oloufa, & Bowie, 2007) Some results from Experiments B through E (see below) were published in the Journal of Management and Engineering Integration. (Bowie, Moslehy, & Oloufa, 2008)

3 Methodology

Because this research project involves the development of a new product, several individual experiments were run as part of the larger research project presented here. Each of these experiments built on the knowledge gained from the previous experiment. Brief descriptions of these experiments are shown in Table 1.

In each experiment, a metal test strip was instrumented by attaching an acoustic sensor. The signal from the sensor was run through a preamplifier that sent the acoustic emission signal on to a computer where the signal was analyzed using acoustic emission software. The acoustic emissions parameters which were collected are described in Table 2.

In order to describe the experimental event accurately, two terms were coined. One “tire bump” (TB) was considered to be one instance of a tire striking the metal test strip. One “axle bump” (AB) was considered to be one instance of an axle (two or more tires) striking the metal test strip. For each TB or AB, several hits are produced. As the tire or axle strikes the metal strip, a hit with a large amount of energy is produced, after which the remaining hits associated with that TB or AB taper off in energy.

Table 1 List of individual experiments

	Date	Location	Config	Research objective
A	Fall 2005	Laboratory test	A	Determine acoustic parameters related to impact force Assess ability to locate point of impact
B	May 2006	Field test (parking lot UCF campus)	A	Evaluate experimental architecture in field environment
C	Fall 2006	Laboratory test	A	Examine relationship between load and acoustic parameters Examine relationship between speed and acoustic parameters
D	Spring 2007	Laboratory test	A	Examine variability of response Examine role of location in response to impact Use two sensors to locate event
E	May 2007, Jun 2007	Field tests (parking lot UCF campus)	A	Examine methods of affixing metal test strip to roadway Examine response to weight and speed in outdoor conditions
F	Jul 2008	Field test (Flagler weigh station)	B	Examine response and variability in real life conditions

Table 2 Description of acoustic emission parameters

Acoustic emission parameter	Description
Rise time (μs)	time elapsed from the beginning of the hit until the peak amplitude is reached
Count	number of times the waveform rises above zero and returns below zero again over the length of the entire hit
Energy (aJ)	energy associated with each hit
Duration (μs)	time length of the hit
Amplitude (dB)	height of the highest peak in each hit
Counts to peak	similar to counts, except it only includes the counts until the peak amplitude is reached
Absolute energy (aJ)	absolute value of the energy in each hit

3.1 Experiment A – Initial laboratory test

3.1.1 Equipment

This experiment used a steel bar with a rectangular cross section as the metal test strip. Two acoustic sensors were attached to the strip (one on each end). The impact was provided in three

different ways: a steel ball dropped from various heights onto the test strip, a pencil lead broken against the test strip, and a bicycle tire rolled across the test strip.

3.1.2 Procedures

To examine the effect of different impact forces on the acoustic parameters, the steel ball was dropped from various heights onto the instrumented metal test strip. Acoustic emission parameters were collected in an attempt to establish the parameter which correlated most closely with impact force. Results for seven different heights were tested, resulting in impact forces of 0.010 J, 0.019 J, 0.029 J, 0.038 J, 0.048 J, 0.057 J, and 0.067 J.

To look at the ability to predict the location of the impact from the difference in time at which the acoustic wave reached each sensor, a lead break test was performed at three locations: one-quarter of the length of the strip, one-half the length of the strip, and three-quarters of the length of the strip. Also, a bicycle tire was rolled across the metal test strip at each of these three locations.

3.2 Experiment B – Field test in UCF parking lot

3.2.1 Equipment

A steel bar with an elliptical top surface was purchased for testing the concept with vehicles on a roadway. For this experiment, sensors were attached to the each end of the bar (see Figure 5). The bar was attached to the roadway surface using duct tape (see Figure 6) and the impact was provided by running a vehicle over the metal test strip. Two different vehicles were used: a pickup truck (see Figure 7) and a compact car (see Figure 8).

3.2.2 Procedures

Each vehicle was driven over the metal test strip at speeds of 5 to 25 mph, providing data points at two different weights and four different speeds.

Figure 5 Sensor attachment to metal test strip

Figure 6 Attachment of metal test strip using duct tape

Figure 7 Pickup truck used for testing, Experiment B

Figure 8 Compact car used for testing, Experiment B

3.3 Experiment C – Laboratory analysis with test apparatus

3.3.1 Equipment

Because of the difficulty in applying different vehicle weights and controlling vehicle speed and the horizontal location at which the vehicle tire strikes the metal test strip, laboratory equipment was developed to provide a controlled environment for Experiments C and D.

3.3.1.1 Construction of the Test Apparatus

Four UCF students in a senior design class designed and built the test apparatus. An inverse design where the roadway rotates and the axis of the tire does not move was chosen for the final design. Figure 9 shows a schematic of the test apparatus.

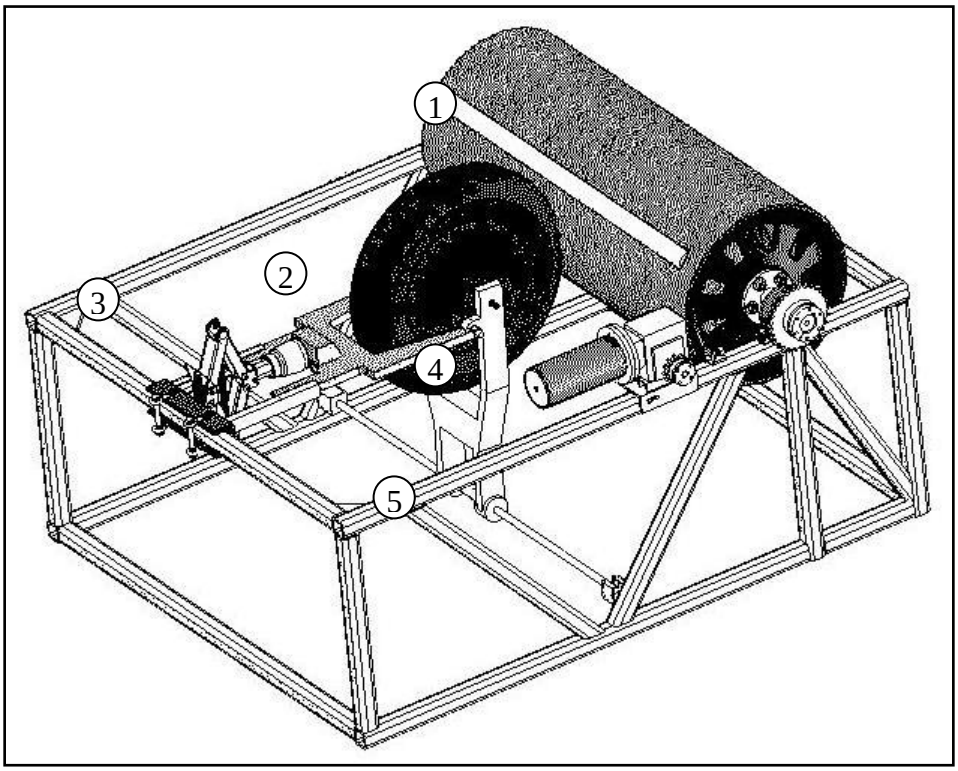

Figure 9 Schematic of laboratory test apparatus

There are five main features of the test equipment, numbered one through five in Figure 9:

1. A rotating cylindrical "road" with the metal test strip attached. The concrete cylinder was constructed of concrete with a 20 inch outside diameter and a 12 inch inside diameter. Automobile tire rims were used as caps for each end of the cylinder. To attach the metal strip, the cylinder was filed down to make a flat surface. The two acoustic sensors were placed 40 inches apart (about 4 inches from each end of the metal strip). For the purposes of lab testing, the sensors were attached using duct tape. The preamplifiers were attached to the wheel rims on either side of the cylinder. Connections from the preamplifiers to the computer run out through the center of the wheel and from there to the computer.

2. A motorcycle wheel. The axis of the wheel does not move, however the wheel does rotate on its axis.
3. A scissor jack which pushes the wheel against the cylindrical "road" at variable weights up to 800 lbs.
4. A motor and reducer which can turn the concrete cylinder at speeds ranging from 0 to 4 mph. Not shown is a bicycle speedometer which measures the speed at which the cylinder turns.
5. A slider and swing arm assembly which allows the location of the motorcycle wheel to be adjusted from side to side.

The UCF mechanical engineering seniors designed and built the entire apparatus (see Figure 10), including pouring and reinforcing the cement for the cylindrical road, cutting and welding the steel for the structural frame, constructing the tensioner, slider, and swing arm, and installing the motor, speedometer, acoustic emission sensors, etc. The testing apparatus went through various validation procedures to ensure it would work as designed. Tests were performed on the power on/off switch, the ability of the motor to drive the cylinder, the ability of the scissor jack to vary the pressure of the tire against the cylinder, the ability to slide the tire from left to right, and the overall ability of the system to run for several minutes at various speeds and loads. The testing apparatus was found to work as predicted in all instances. For Experiment C, only one sensor was used.

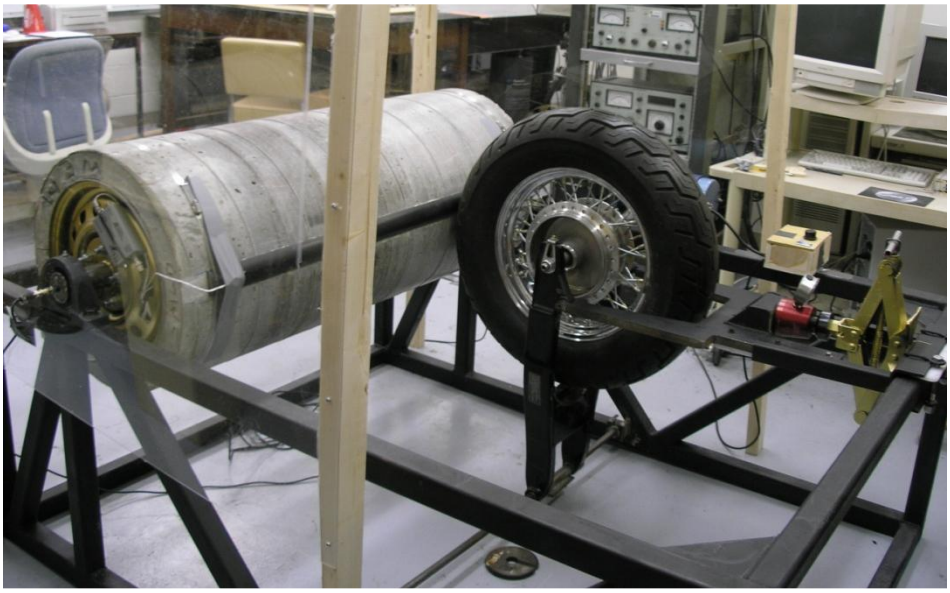

Figure 10 Photograph of laboratory test apparatus

3.3.2 Procedures

Forty-two separate experiments were run at 14 different levels of weight – from 100 to 750 lbs in 50 lb increments – and three different levels of speed – approximately 2, 3, and 4 mph. Each experiment involved collecting data for 30 consecutive TBs at each combination of weight and speed.

3.4 Experiment D – Continuation of laboratory testing

3.4.1 Equipment

The equipment for Experiment D was the same as that used for Experiment C, except that both sensors were used. Also, the metal test strip was filed flat under the sensors to provide a better contact surface.

3.4.2 Procedures

For this set of experiments, the speed was held constant at 3 mph, the tire impact location was varied between 10 inches, 20 inches, and 30 inches from sensor one (corresponding to 30 inches, 20 inches, and 10 inches from sensor two), and the load was varied between 500, 600, 700, and 800 lbs. At each of the twelve settings, 30 repetitions of the experiment were performed. For each repetition, the acoustic emission output was collected for one TB.

An additional experiment attempted to use two sensors to determine the horizontal location of a TB along the metal test strip. First, the speed of sound in the strip was calibrated. This was done with a lead break test. The pencil lead was broken against the metal test strip on the outside of each sensor. Using the time at which the sensors detected a hit and the length between the sensors, the speed of sound in the metal test strip was determined. The AEWin software can then calculate the location of an event (such as a TB or a lead break) based on the time difference at which the hits arrive at the two sensors.

3.5 Experiment E – Additional field testing in UCF parking lot

3.5.1 Equipment

The metal test strip and sensors were the same as those used in Experiment B. On the test day in May 2007, the metal test strip was attached to the roadway using duct tape (see Figure 11). On the test day in June 2007, the metal test strip was attached to the roadway using epoxy. The test vehicle was a Sierra GMC truck, with a curb weight of approximately 4,000 lbs. The weight of the test vehicle was varied by adding passengers and sandbags, with a maximum weight of approximately 5,000 lbs.

3.5.2 Procedures

In May 2007, two speed conditions (10 mph and 20 mph) and two weight conditions (approximately 4,000 lbs and 4,700 lbs) were tested. In June 2007, three speed conditions (10 mph, 20 mph, and 30 mph) and three weight conditions (approximately 4,000 lbs, 4,500 lbs, and 5,000 lbs) were tested. Only one test run at 30 mph was performed because this speed seemed unsafe in the geometry of the parking lot.

Figure 11 Metal test strip duct taped to road surface (May 2007)

3.6 Experiment F – Field test at Flagler Weigh Station

3.6.1 Equipment

New equipment was purchased or developed for this experiment. New sensors were purchased (Pico HF-1.2 sensors sold by Physical Acoustics Corporation). These sensors were chosen because of their small size (0.2 inch diameter by 0.15 inch height) and wide frequency range (500 to 1850 kHz). In addition, the metal test strip that had been used in previous experiments was cut in half (with each piece now measuring approximately 75 inches in length) and a groove was machined from the bottom surface to allow the sensors to be embedded in the test strip and to provide protection for the cables from the sensors to the computers. Figure 12 shows the sensor attachment to the underside of the test strip with a cable running through the groove. Prior to machining the metal test strip, a stress analysis was performed. The stress analysis determined that the metal test strip would withstand the weight of a fully loaded commercial truck under the new configuration (see Appendix).

Epoxy was used to affix the metal test strip to the road surface. The metal test strip was attached to the road surface on the ramp leading from I-95 to the Flagler weigh station, just downstream of the permanent WIM sensors installed at the weigh station. Figure 13 shows a schematic of the experimental set up and a photo is shown in Figure 14. Figure 15 shows how the sensors were connected to the computer via a preamplifier.

3.6.2 Procedure

Setting up the test equipment just downstream of the installed WIM system allowed direct comparison of the WIM output and the acoustic emission response. For each vehicle, the installed WIM equipment provided information on: distances between axles, half and full axle weights for each axle, vehicle class, vehicle length, width, height, speed, and a unique record number. For approximately 70 commercial vehicles that traveled through the weigh station, the WIM output was printed and the acoustic emission response was collected by the computer. The record number was used to associate the WIM output with the acoustic emission response.

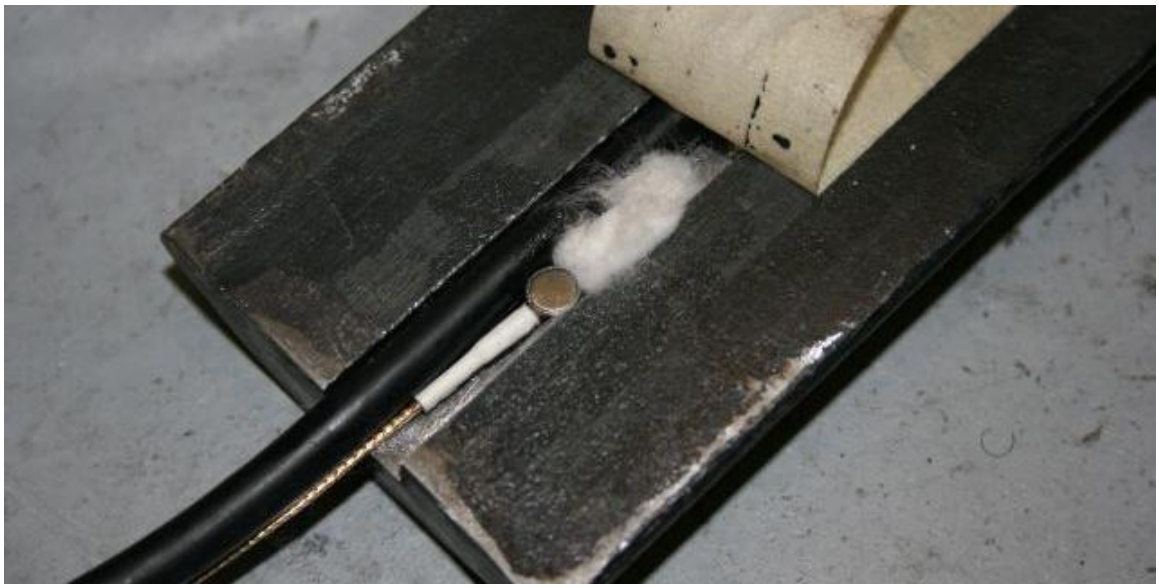

Figure 12 Minisensor attachment (bottom side of metal test strip)

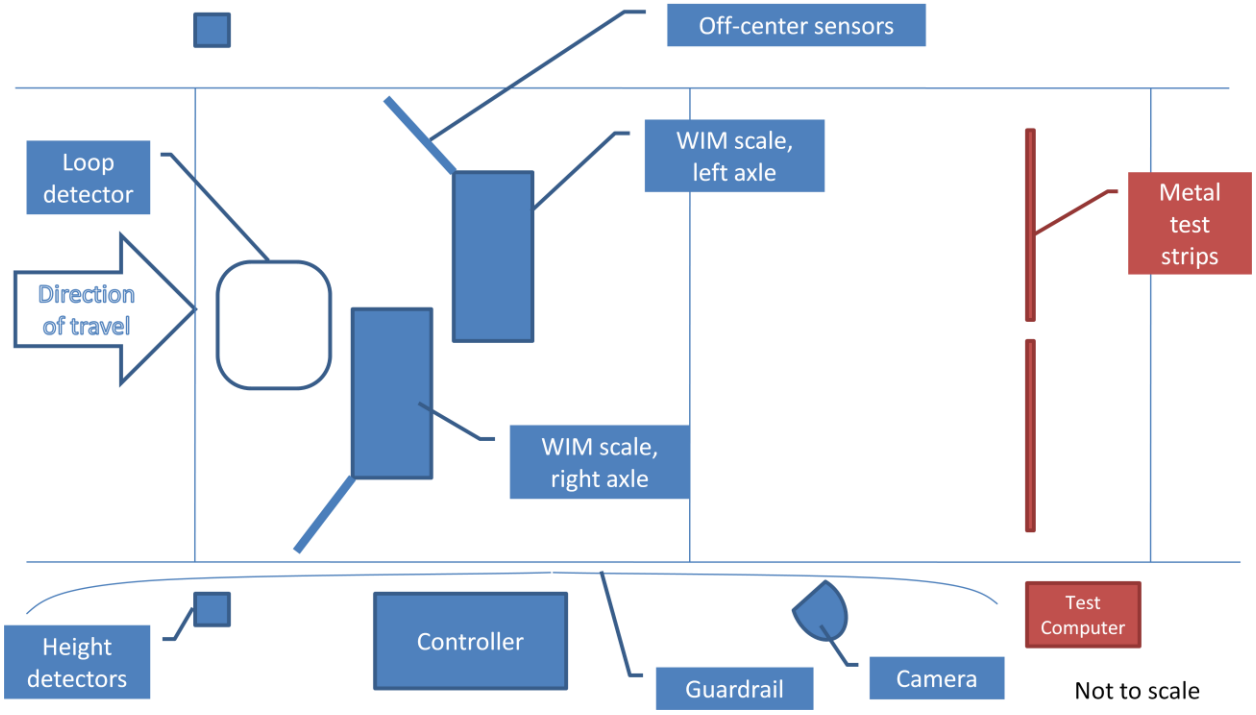

Figure 13 Schematic of WIM equipment installed at Flagler weigh station and experimental equipment

Figure 14 Photo of WIM equipment installed at Flagler weigh station and experimental equipment

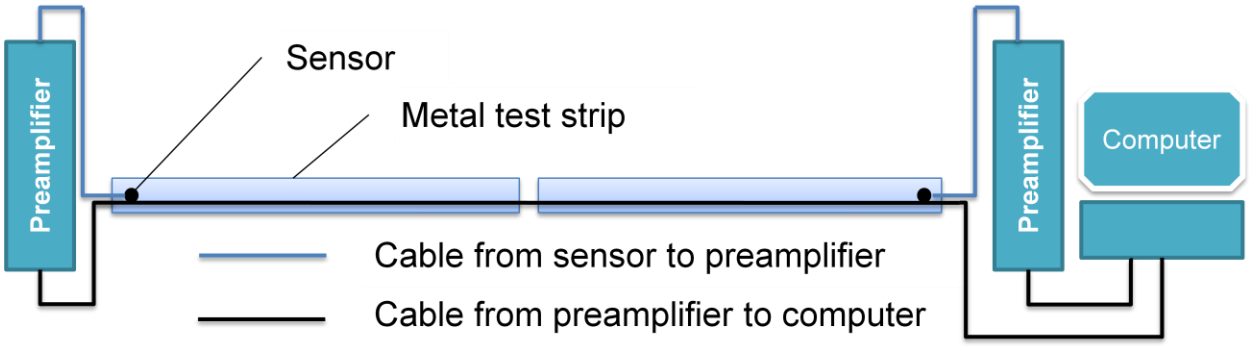

Figure 15 Schematic of connections from sensors to computer

3.7 Acoustic emission data preparation

In each of the six experiments described above, AEWin software was used to record the acoustic emission response detected by the sensors. The software separates the response into "hits." A hit is defined as the waveform between when the acoustic sensor output exceeds some pre-determined amplitude, the output amplitude peaks, and then the acoustic sensor output goes back below the threshold amplitude. For more simple events (such as a pencil lead breaking against the metal strip), only one or two hits are produced per event. However, for the more complex event of a tire rolling across the metal strip, many hits are produced for each TB.

The software records the acoustic emission parameters for each hit, including time (the amount of time that has passed from when the recording began), channel (corresponding to which sensor detected the hit), rise time, count, energy, duration, amplitude, counts to peak, and absolute energy (see Table 2 for descriptions of these parameters). This line by line list of all of the parameters for each hit in a recording was imported into Microsoft Excel to facilitate analysis of the data.

4 Findings

As the experiments each had a different objective, the findings of each experiment are reported separately in the following sections.

4.1 Experiment A – Initial laboratory test

For the ball striking the metal test strip, a linear correlation between the impact force and the absolute energy of the acoustic emission response was detected. Figure 16 shows the results for sensor one and Figure 17 shows the results for sensor two.

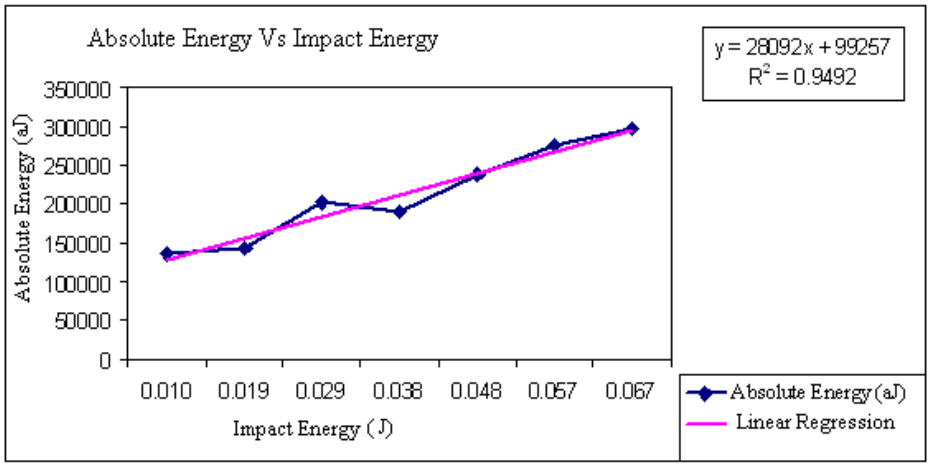

Figure 16 Correlation of impact force and acoustic response for sensor one

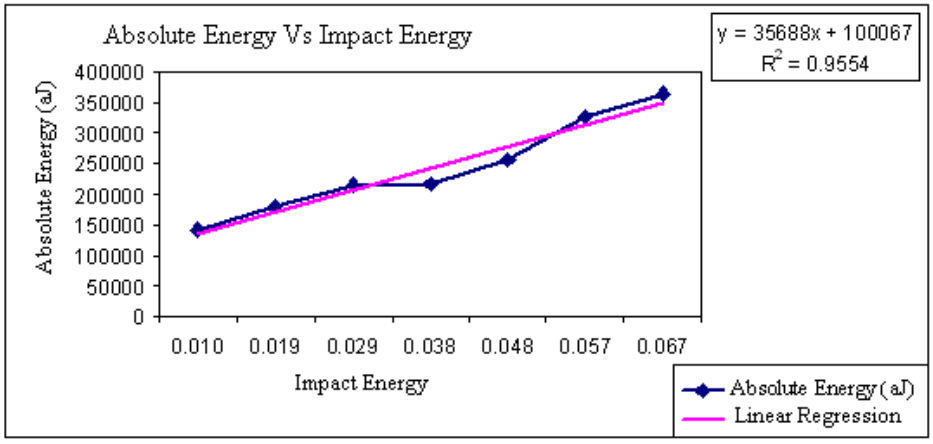

Figure 17 Correlation of impact force and acoustic response for sensor two

Results of the lead break and bicycle tire tests showed that the location of impact could be predicted (see Table 3).

Table 3 Results of lead break and bicycle tire tests

	Actual Location (in)	Predicted Location lead break (in)	Predicted Location bicycle tire (in)
25%	22.25	22.85	30.77
50%	44.5	46.64	42.45
75%	66.75	66.74	72.01

4.2 Experiment B – Field test in UCF parking lot

The speed of the truck was computed from the time between the ABs and a knowledge of the distance between the axles (116 inches). The results for different speeds are summarized in Table 4.

Table 4 Comparison of actual and computed speed of pickup truck

Speedometer reading (mph)	Computed speed (mph)
5	4.2
10	12.4
20	19.4
25	24.4

In addition to the acoustic emission parameters, the wavelet coefficient was also determined. Figure 18 shows a 3-D plot of the wavelet coefficients. Plotting the maximum value of the wavelet coefficient for different truck speeds yielded Figure 19, which shows a correlation between the speed of the truck (same weight) and the computed maximum wavelet coefficient.

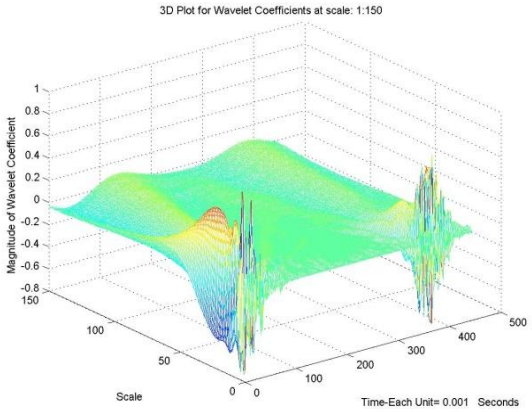

Figure 18 3-D plot of wavelet coefficients

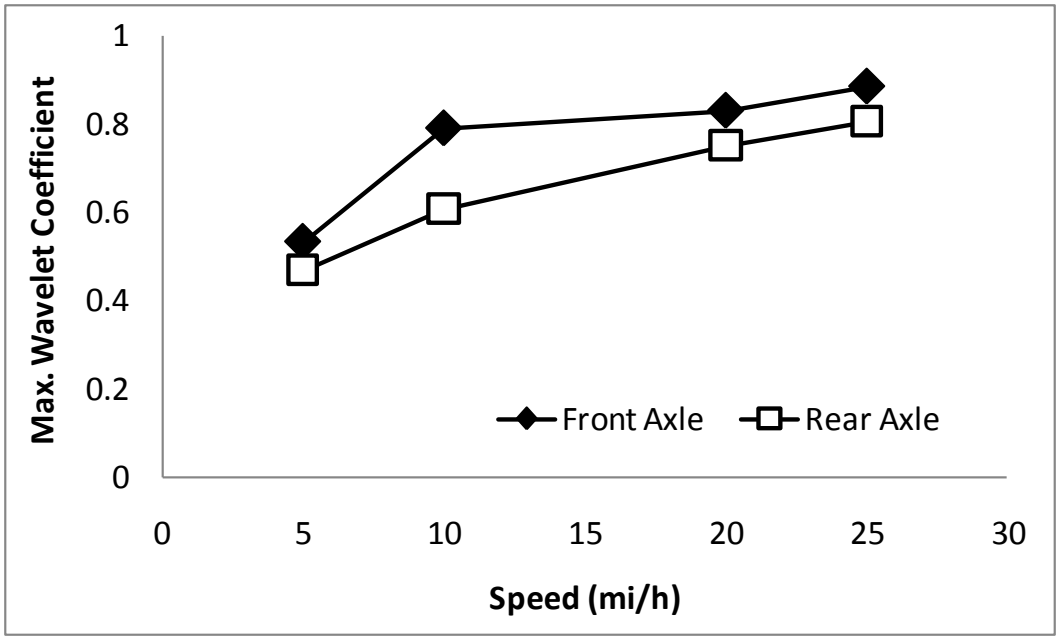

Figure 19 Correlation between maximum wavelet coefficient and truck speed

4.3 Experiment C – Laboratory analysis with test apparatus

The purpose of this experiment was to determine which of the acoustic emission parameters correlate with weight and to find some way to quantify the correlation. With each set of 30 TBs, an average of about 130 hits was collected. About 3 in 4 of these hits were "residual" in nature, with very low values of the acoustic emission parameters. As a result, the residual hits caused the average values of the 130 hits over the 30 TBs to skew low and no correlation was found between the acoustic emission parameters and the load.

The first attempt at separating the hits of interest from residual hits was to look for a threshold value for one of the acoustic emission parameters that could be used to filter out the residual hits and isolate one hit of interest for each TB. The acoustic emission parameter "count" was found to work best as a filter for isolating hits of interest; however, even for this parameter, different threshold values were needed depending on the load and the speed. Therefore, filtering using a threshold value was rejected as a reliable means of isolating hits of interest.

Eventually, it was found that for several acoustic emission parameters, the maximum hit produced with each run of 30 TBs was correlated with weight. For instance, Figure 20 shows count as a function of load. When an average of all of the hits over the 30 TBs at each load is graphed (the diamonds in the figure), no correlation with load is found. When the maximum hits for each TB is isolated, however, a distinct trend of increasing count with increasing load up to about 400 lbs is shown (the triangles in the figure).

Similar trends were found when energy and absolute energy were considered. Figure 21 shows a distinct trend of increased energy with increased load when the maximum hit for each TB is isolated. Figure 22 shows similar results for absolute energy. No correlation was found between the parameters rise time, counts to peak, duration, or amplitude and load.

Speed did not appear to affect the acoustic emission parameters very much; however, it should be noted that the differences in the speeds were very small. In other experiments (see section 4.5) where speed differences were greater, larger changes in acoustic emissions with speed were noted.

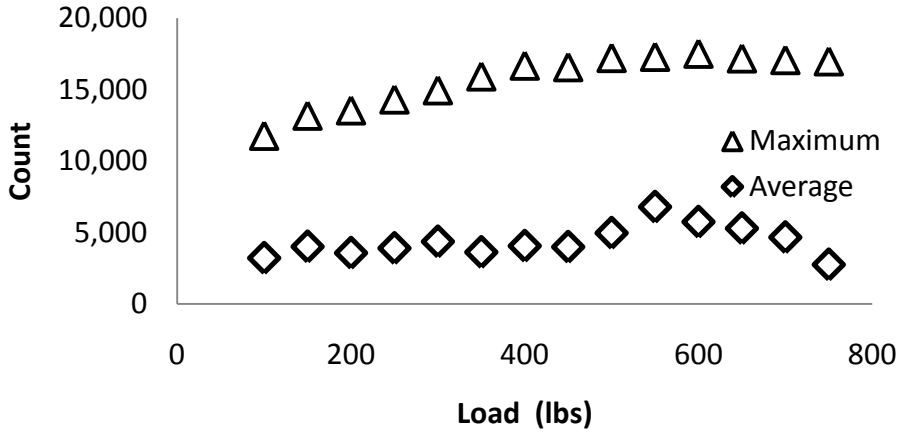

Figure 20 Count as a function of weight

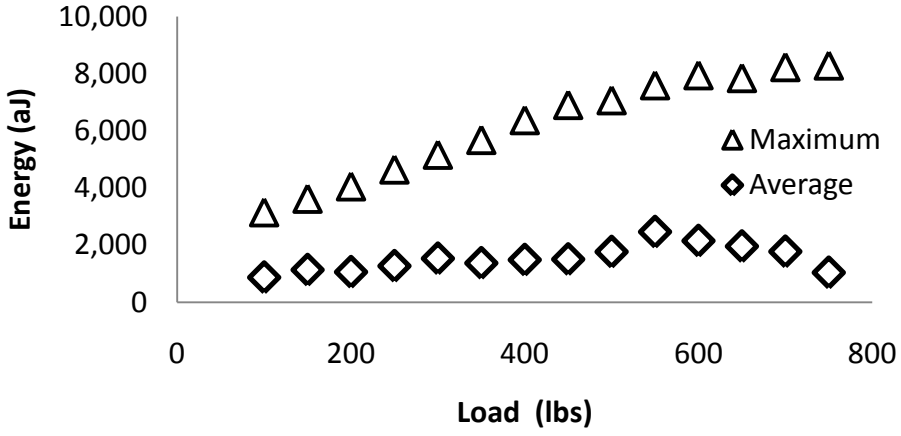

Figure 21 Energy as a function of weight

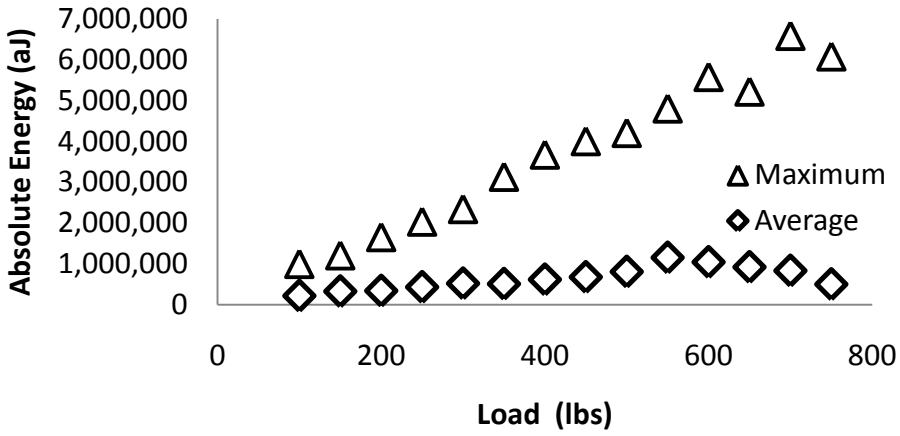

Figure 22 Absolute energy as a function of weight

4.4 Experiment D – Continuation of laboratory testing

Having established that count, energy, and absolute energy were correlated with load in the last experiment, this experiment looked at each TB individually so that variability in the data could be examined. In addition, other methods of dealing with the residual hits and the effect of the location of the TB were examined.

4.4.1 Graphical methods

The previous experiment had shown that average values of count, energy, and absolute energy for all of the hits associated with a TB did not correlate with load, but that the maximum values did. To further examine the best method of correlating the acoustic emission output to load, the sum of all of the hits associated with a TB was examined using this new data set. Figure 23 shows the value of the sum of energy over each TB for the 360 TBs collected in this data set. (Note that only values for channel 2 are shown, because channel 1 was not working properly when the data were collected.) In the graph, there is a clear correlation between the sum of the energy and load as well as between the sum of the energy and location. Similar correlations can also be seen in Figure 24 through Figure 26, which are graphs showing the maximum values of energy, the sum of count values, and the maximum values of count for the data set, respectively. Figure 27 and Figure 28 show no clear pattern for absolute energy.

4.4.2 Regression analysis

To further explore the relationship between acoustic emission parameters, load, and location, a regression analysis was performed using the data. The regression analysis showed that many of the acoustic emission parameters were useful in developing a model for load based on location and acoustic emission parameters. Table 5 shows two possible models, one fairly complicated model and one very simple model. The more complicated model fits the data fairly well, with an adjusted R^2 value of 73%. The adjusted R^2 for the simpler model is 35%. In both cases, the variability of the model is fairly high, with residuals of ± 150 lbs even for the more accurate model. Figure 29 is a histogram of the residuals for the two models. Model A is clearly the better model, with a narrower band of residuals.

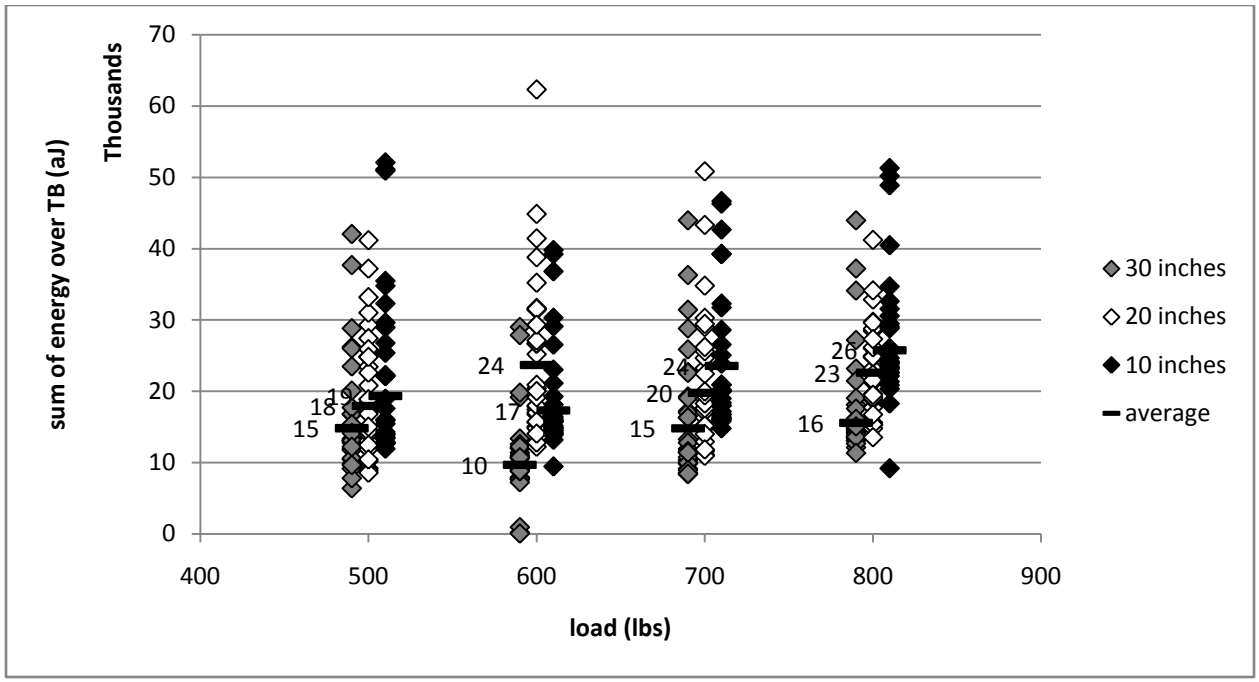

Figure 23 Sum of energy over the TB by location

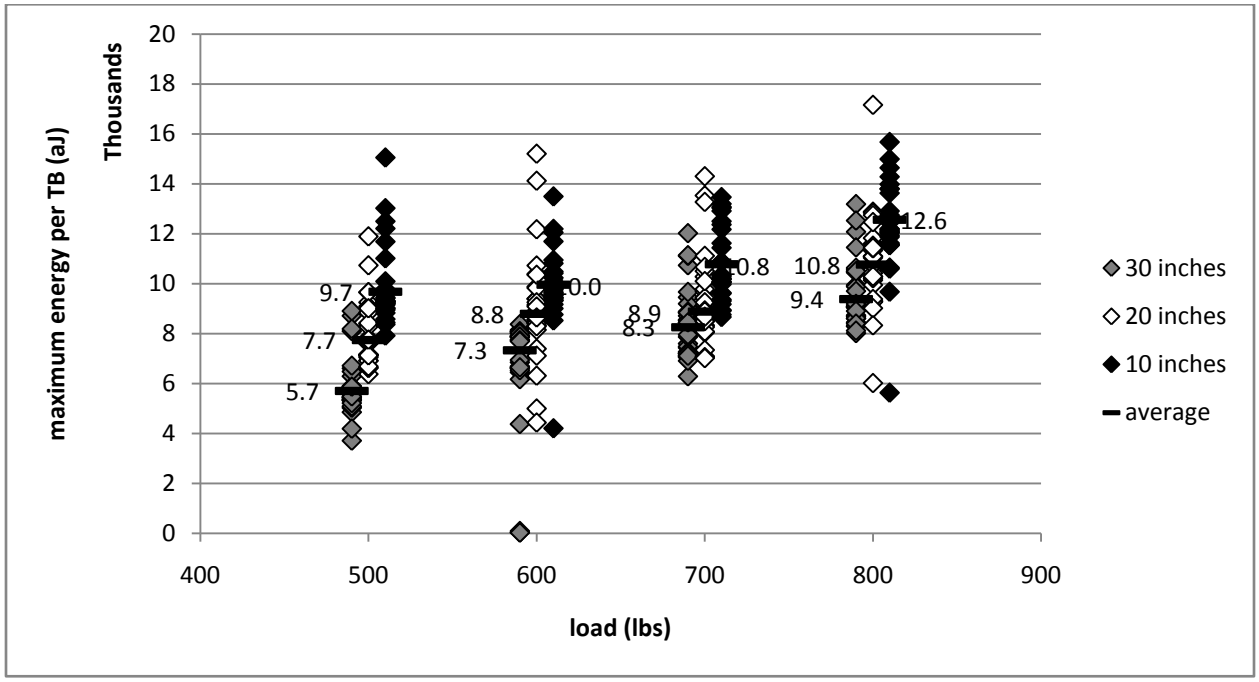

Figure 24 Maximum energy per TB by location

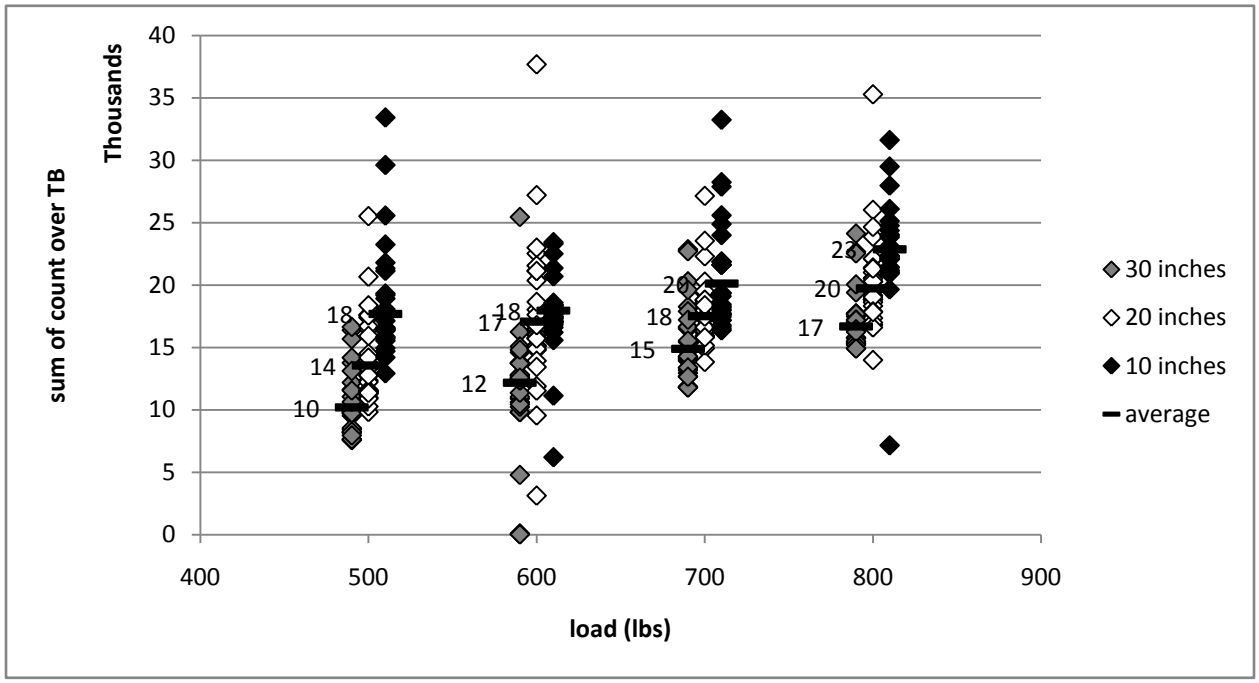

Figure 25 Sum of count over the TB by location

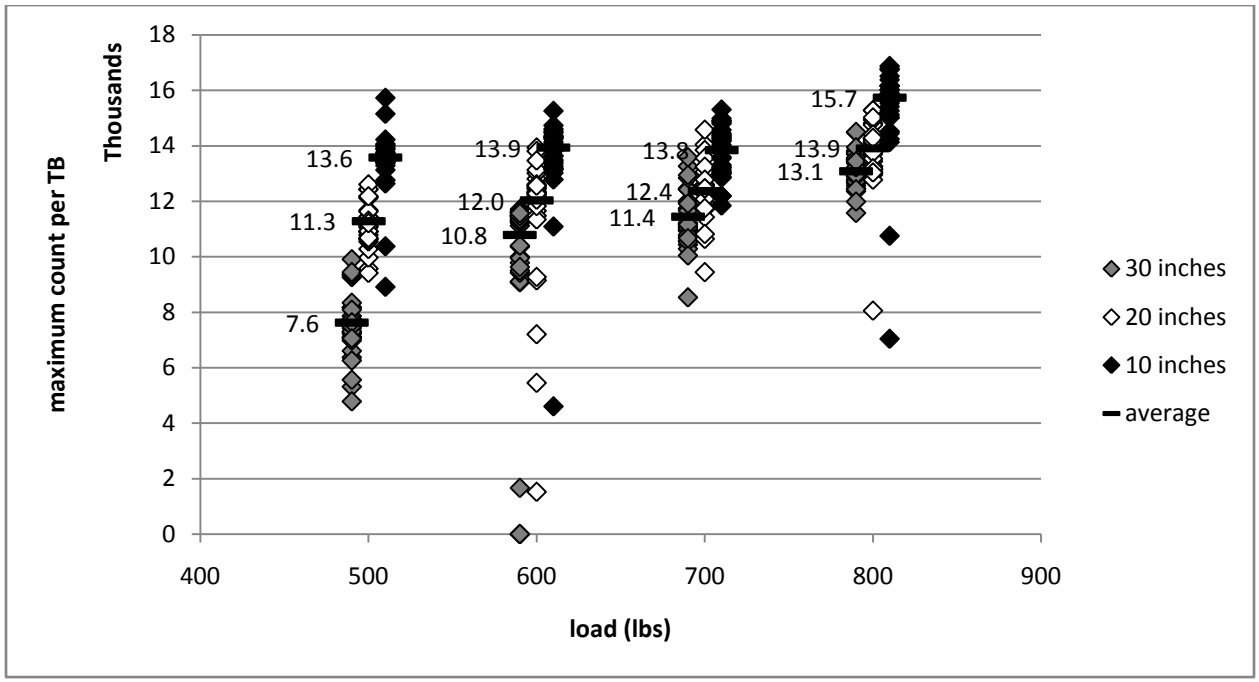

Figure 26 Maximum count per TB by location

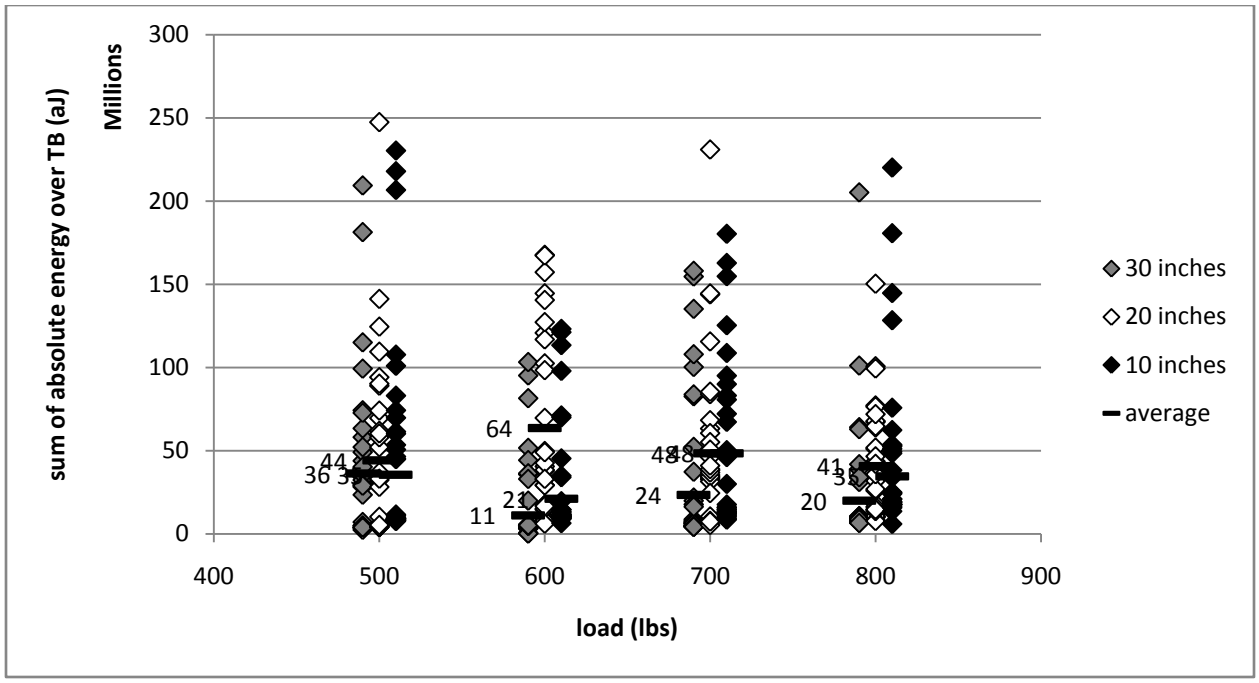

Figure 27 Sum of absolute energy over the TB by location

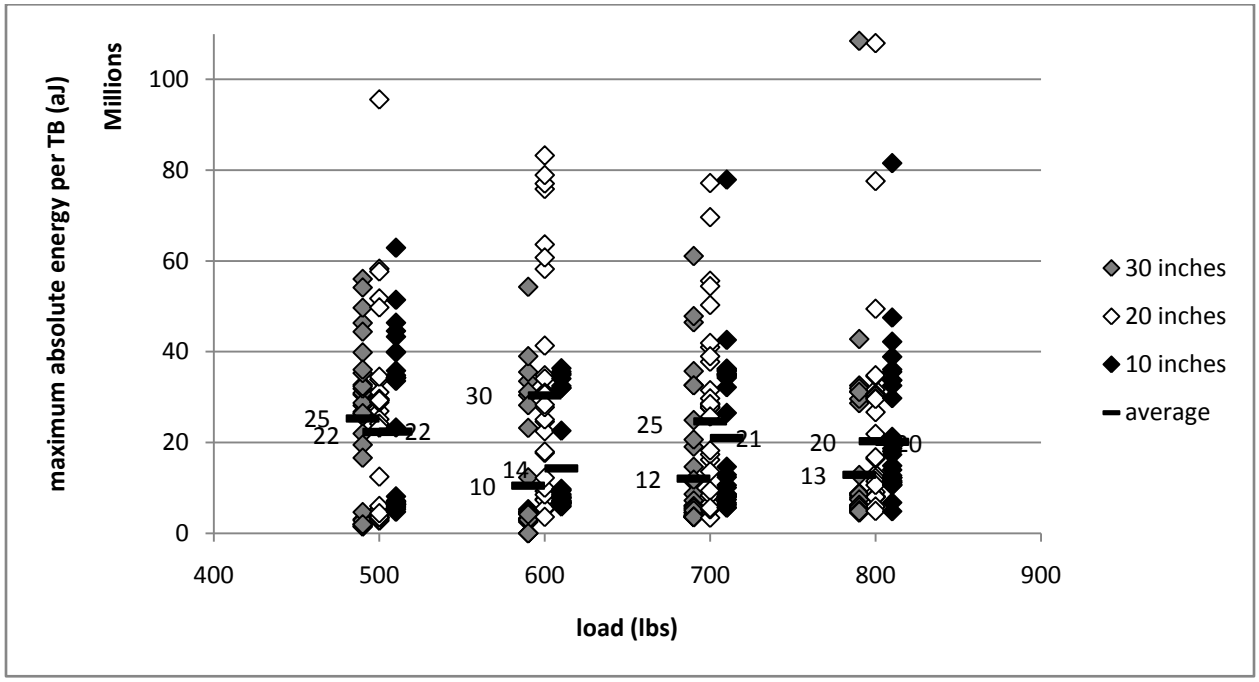

Figure 28 Maximum absolute energy per TB by location

Table 5 Models for load from laboratory experiment D

	Model	adjusted R^2
A	$load = 691 - 10 \times location - 0.00000032 \times absolute\ energy\ sum + 0.048 \times count\ to\ peak\ sum + .01005 \times \max\ energy + 0.0305 \times \max\ count - 0.00355 * \max\ duration - 0.052 \times \max\ count\ to\ peak$	73%
B	$load = 450 - 5.14 \times location + 0.0327 \times \max energy$	35%

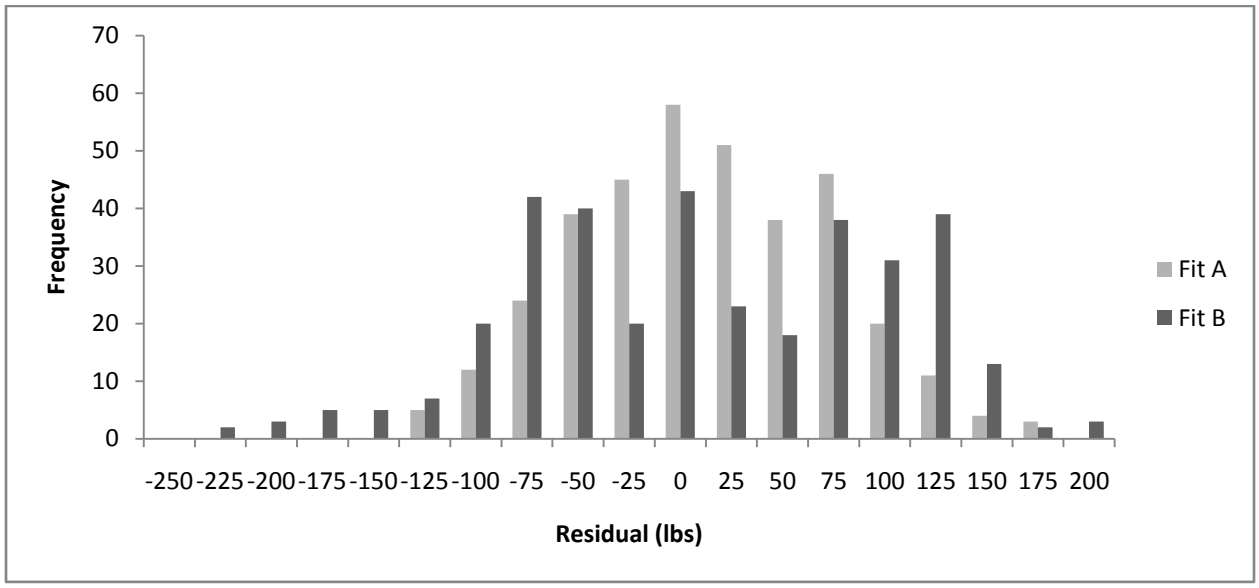

Figure 29 Histogram of the residuals for the fits of models A and B, experiment D

Because of the high variability in the acoustic emissions data, the laboratory equipment was examined to determine if any sources of variability could be reduced or eliminated. Several changes were implemented, including improving the seating of the sensors onto the metal test strip, reversing the direction of rotation of the concrete cylinder "road," and reinforcing the electrical connections from the sensors to the computer (the rotation had placed these connections under considerable stress). These measures did reduce the variability of the data (see Figure 30, which shows the residuals for a model fitting the new, lower variability data compared to the residuals for model A above), but the stress on the laboratory equipment was such that a repetition of the data analysis performed before these changes were made could not be repeated. It was concluded that further testing should be performed in the field, where some of the sources of variability would be reduced or removed.

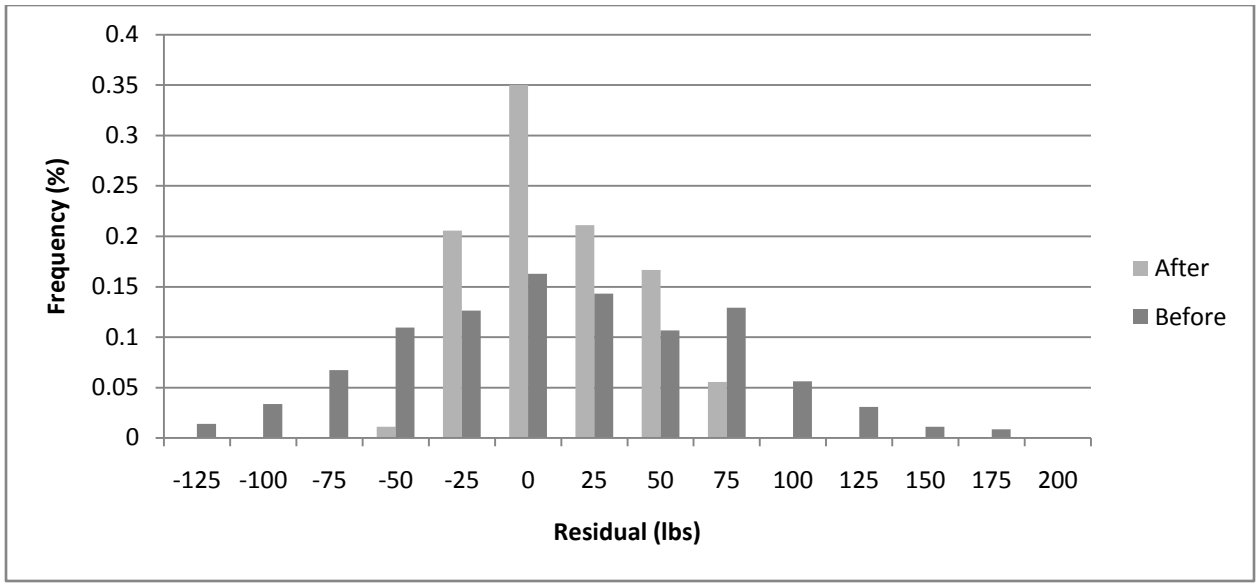

Figure 30 Histogram of residuals showing reduced variability, experiment D

4.4.3 Event location

The speed of the sound wave in the metal test strip was found to vary from as slow as 178,000 inches per second to as fast as 197,000 inches per second, perhaps depending on temperature. When calibrated correctly, the AEWin software was able to accurately determine the location of a simple event such as a lead break test. However, the large number of hits generated by a complex event made it impossible for the software program to accurately deduce the originating location of a complex event such as a TB.

4.5 Experiment E – Additional field testing in UCF parking lot

One purpose of this set of experiments was to examine how the method of affixing the metal test strip to the road surface affects the acoustic response. When the metal test strip was affixed using duct tape, the strip was observed to bounce up and down as the vehicle passed over it, resulting in higher maximum values for count, energy, and absolute energy. When the strip was affixed using epoxy, it remained attached to the pavement along its entire length and the maximum hit values for count, energy, and absolute energy were lower (see Table 6).

Additionally, correlations were found between the acoustic emission parameters and speed, but no correlations were found between any of the acoustic emission parameters and weight. As mentioned in section 4.3, it appears that the difference between this finding and the laboratory test findings may be caused by differences in relative variation in load level and speed. In the field tests, the relative variation in load was small (1,000 to 1,250 lbs per wheel) and the relative variation in speed was high (10 mph to 30 mph), whereas in the laboratory the relative variation in the load was large (100 lbs to 750 lbs) and the relative variation in the speed was small (2 mph to 4 mph).

Because the pickup truck used in the experiment has two axles, during one repetition of the experiment, two ABs are collected, referred to as AB 1 (front axle) and AB 2 (rear axle).

Figure 31 shows the typical pattern of hits collected during one repetition of the experiment. Note that the vibrations from the vehicle striking the metal strip remain for some period after the vehicle has completely passed. The time from when the vehicle first strikes the metal strip until these vibrations have died away is known as the acoustic emission duration.

A correlation was found between the acoustic emission duration of each run and the speed of the vehicle. Figure 32 shows the values of these variables for each run and the averages for 10 mph and for 20 mph.

Table 6 Comparison of maximum hit values by method of affixation for empty pickup truck

	Duct tape			Epoxy		
	Energy (aJ)	Absolute energy (aJ)	Count	Energy (aJ)	Absolute energy (aJ)	Count
10 mph	30,000	307,000,000	19,000	200	38,000	15
20 mph	37,000	241,000,000	14,000	400	72,000	40

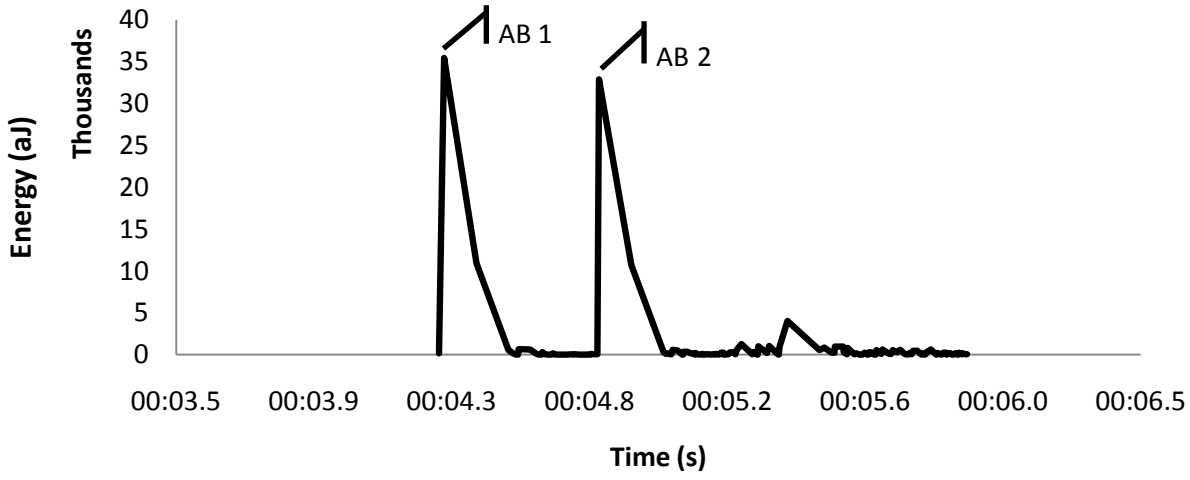

Figure 31 Typical pattern of energy in hits during one repetition (2 ABs)

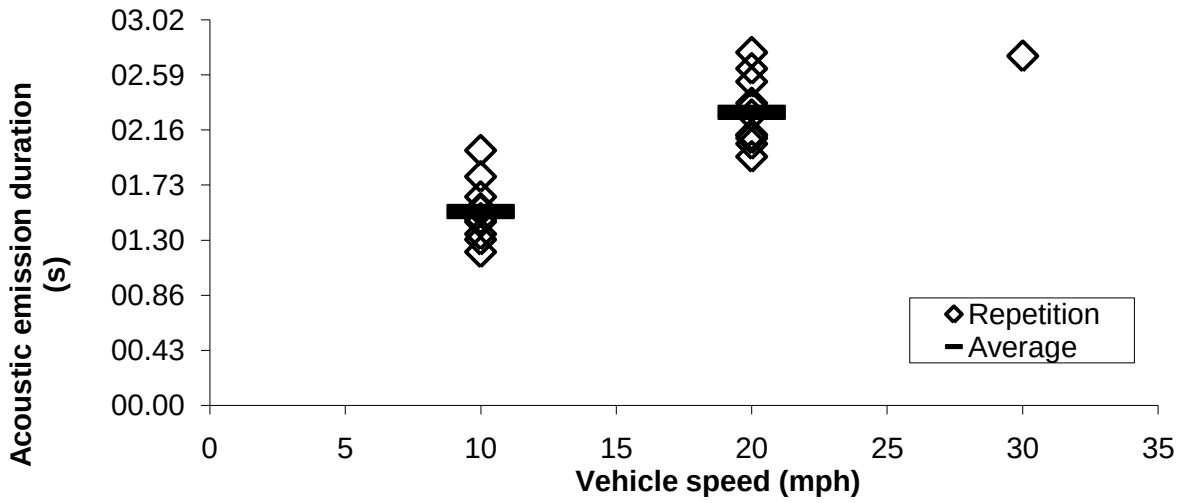

Figure 32 Acoustic emission duration as a function of truck speed

4.6 Experiment F – Field test at Flagler Weigh Station

4.6.1 Difficulties with equipment

During the testing at Flagler Weigh Station, there were repeated problems with the PCI card not being detected by the AEWin software. This was repaired several times by reseating the card and reinstalling the driver software. However, after about two hours of data collection none of these strategies worked and data collection had to end. When the system was tested the next day after it had been moved inside, the card was easily detected by the software. This leads to the conclusion that the PCI card was adversely affected by the heat during outdoors operation. Future configurations of the equipment need to be more resistant to effects of the weather.

4.6.2 Data preparation

The acoustic emission response was recorded for 109 trucks passing over the test equipment and the WIM output was printed out for 124 trucks passing over the WIM equipment; however, due to operator error or equipment failure, there were only 69 trucks for which both the acoustic emission response and the WIM output was recorded. General characteristics of these 69 trucks are shown in Table 7. The minimum truck speed was 24 mph and the maximum speed was 46 mph. The minimum gross weight was 9,600 lbs and the maximum gross weight was 110,700 lbs.

The first step in the data analysis was to identify the time location of the ABs in the acoustic emission response. Figure 33 shows the energy of each hit with time for vehicles of three different classes. The AB time locations were first calculated using the speed and distance between axles reported by the WIM. Then, visual inspection was used to confirm the time locations. Once the ABs were located for each vehicle, the maximum values of the acoustic parameters from the beginning of one AB to the beginning of the next AB was determined. Because a separate acoustic emission response and a separate axle weight from the WIM was recorded for the left and right side of each AB, this resulted in a total of 612 half axle weight (HAW) records.

Table 7 General characteristics of 69 recorded trucks

Vehicle class	Frequency	Average speed (mph)	Average gross weight (lbs)
3	2	38.5	16650
4	6	35.8	31183
5	4	34	16575
6	1	39	55300
7	0	N/A	N/A
8	5	38.4	34120
9	48	38.1	57454
10	2	34.5	105300
11	1	35	39800

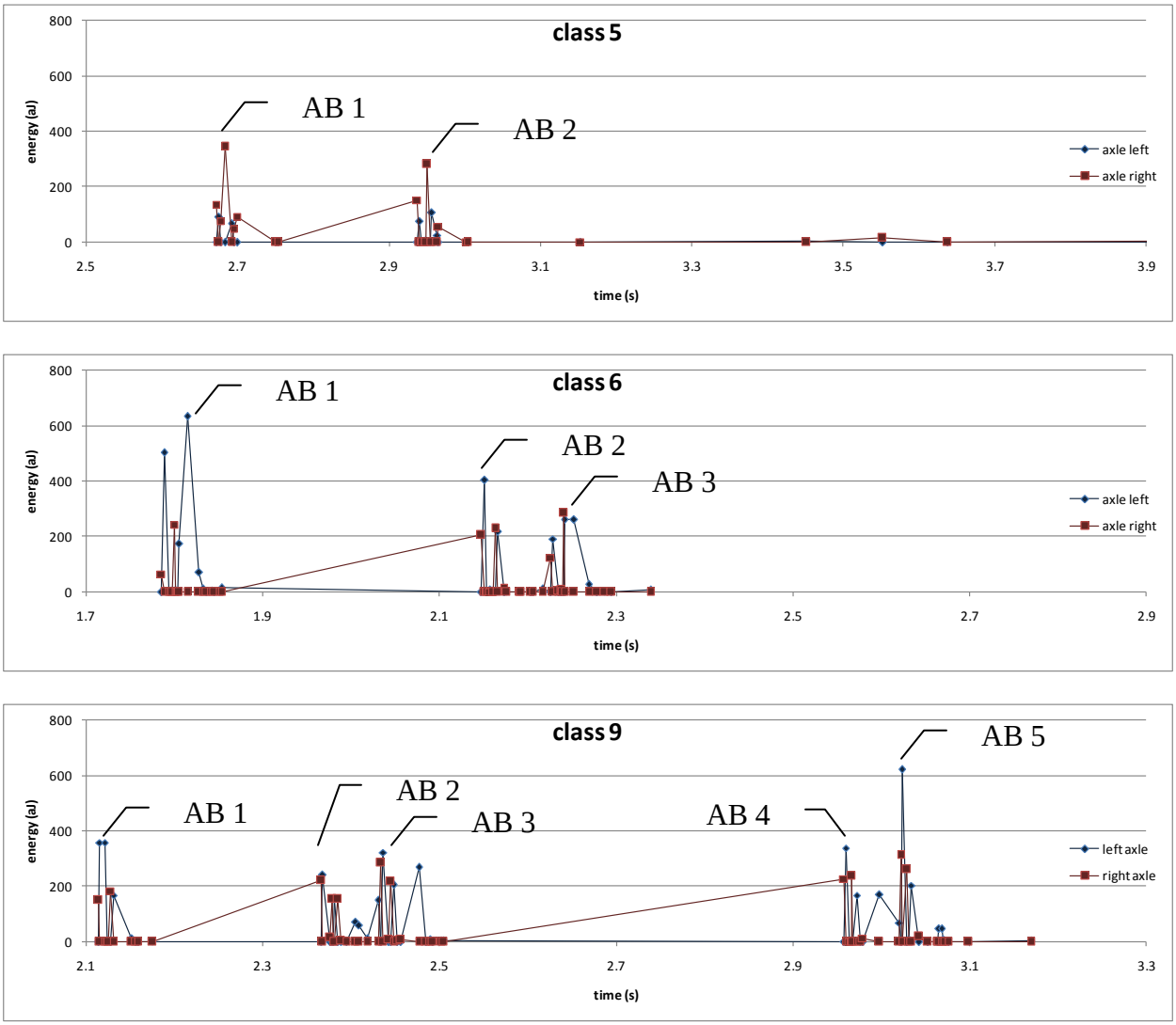

Figure 33 Acoustic emission energy response with time for three different vehicles.

In addition to visually inspecting the data to determine the location of the ABs, the data was visually inspected to remove hits with extreme values that did not occur at the onset of the AB. Eight hits were removed during this process, resulting in more reasonable maximum acoustic response values being recorded for these ABs.

Even though the sum of the acoustic emission values over an AB had been shown to be related to load in Experiment D, the sum was not used in this analysis for two reasons. First, for tandem axles, the acoustic emission response from one AB did not have time to die out before the following AB occurred. Second, the subjective nature of the determination of the starting and ending point of an AB would make the sum an inaccurate measure.

4.6.3 Development of the statistical model

After visual inspection of the energy of the raw hits was complete, the data were brought into Minitab for statistical analysis.

4.6.3.1 Transformations of explanatory variables

A matrix plot of the actual HAWs plotted against each of the acoustic emission parameters revealed that the relationship between the HAW and most of the acoustic emission parameters was not linear. Therefore, a logarithmic transformation was performed on all of the acoustic emission parameters except for amplitude (for which no relationship with HAW was detected). Figure 34 is a matrix plot showing the relationship between the actual HAWs and the transformed parameters.

4.6.3.2 The role of speed in the model

Obviously, the actual HAW as measured by the WIM is the response to be predicted by the model. However, speed also clearly affects the acoustic emission parameter values and therefore must be included in the model. Three possible scenarios for including speed were envisioned:

1. The response is HAW and speed is included as one of the explanatory variables.
2. The response is momentum, represented by HAW x speed.
3. The response is kinetic energy, represented by HAW x speed^2.

4.6.3.3 Unusual data points

When performing regression analysis, Minitab highlights data that is unusual either because of large residuals or high leverage. Many of these points were examined more closely; however, the model was not significantly improved by removing these points, so the final model presented here includes all 612 data points.

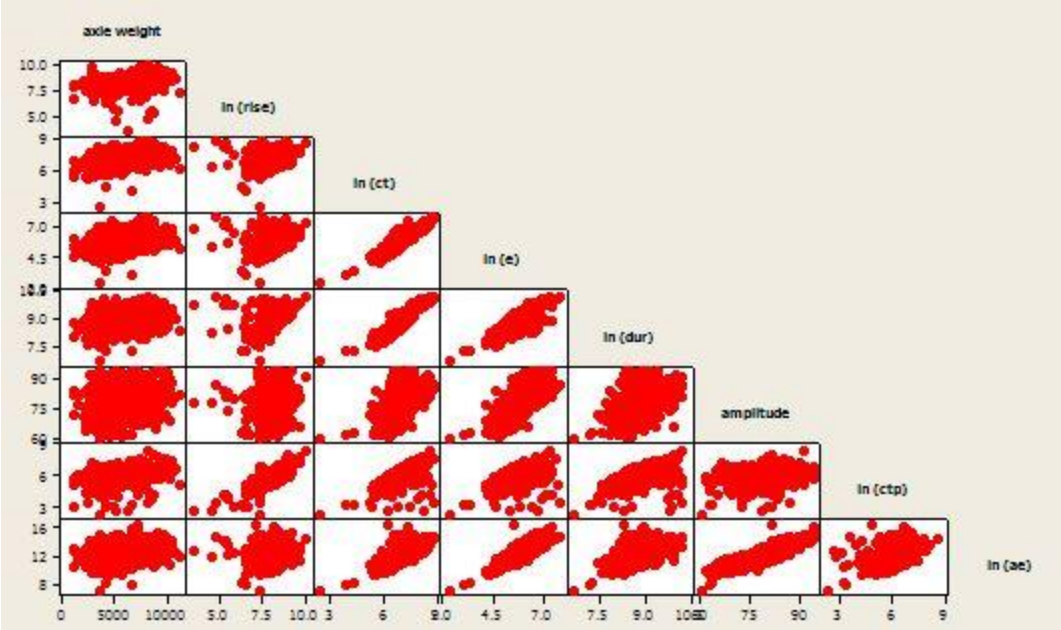

Figure 34 Matrix plot of transformed acoustic emission parameters and half axle weight

4.6.3.4 Final model selection

For each of the response variables listed in section 4.6.3.2 above, a stepwise regression was performed to determine which of the acoustic emission parameters was most helpful in modeling the HAW. In addition, a regression analysis was performed using only the most pertinent acoustic emission parameter. This resulted in six possible models, three relatively complex and three relatively simple. The six models are presented in Table 8.

Table 8 Selected models for HAW

		Model for HAW	adj R^2
[A]	ln(HAW)	$haw = e^{11-0.206speed+0.00271speed^2+0.0674\ln(ctp)+0.178\ln(energy)}$	21.2%
[B]	HAW	$haw = 21399 - 1183speed + 15.6speed^2 + 1120\ln(energy)$	21.9%
[C]	HAW x speed	$haw = \frac{-54276+21683\ln(abs.energy)+17878\ln(ctp)-13316\ln(rise)}{speed}$	17.3%
[D]	HAW x speed	$haw = \frac{-80527+24028\ln(abs.energy)}{speed}$	16.6%
[E]	HAW x speed^2	$haw = \frac{3412407+1218701\ln(abs.energy)-2088056\ln(dur)+1195483\ln(ct)}{speed^2}$	19.7%
[F]	HAW x speed^2	$haw = \frac{674105\ln(abs.energy)}{speed^2}$	N/A

4.6.4 Adequacy of the models

The adjusted R^2 values for the six models are not very high – to develop a more complete model, other parameters would need to supplement the acoustic parameters shown here. Nevertheless, the following graphs show that these models show promise for determining gross vehicle weight.

For Figure 35 through Figure 40, the black circles represent the actual HAWs measured by the WIM scale. Each figure additionally shows the fit HAWs, determined using one of the above models, A through F. In looking at these figures, there are a few interesting observations:

- In the simpler models (B, D, and F), the data seem to be grouped in bands according to speed. This is because speed is one of the few parameters in these models and the speed data were reported in integer values. The actual axle weights do not group themselves in bands according to speed.
- The predictions of the kinetic energy models (E and F) are generally too high.
- There is not much difference between the predictions for the HAW models (A and B) and the momentum models (C and D).

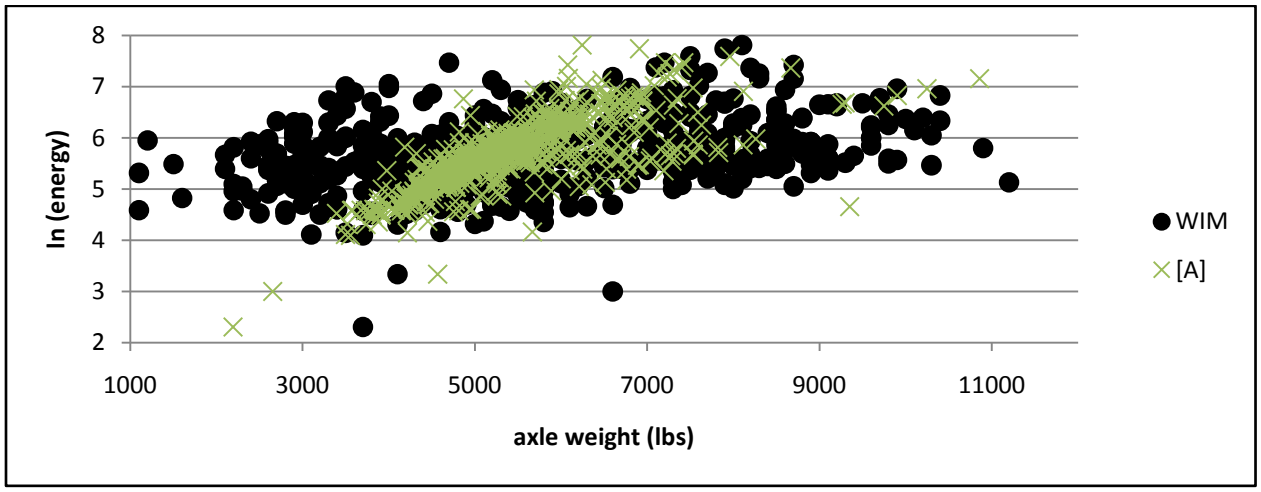

Figure 35 Model A – axle weight as a function of ln(energy)

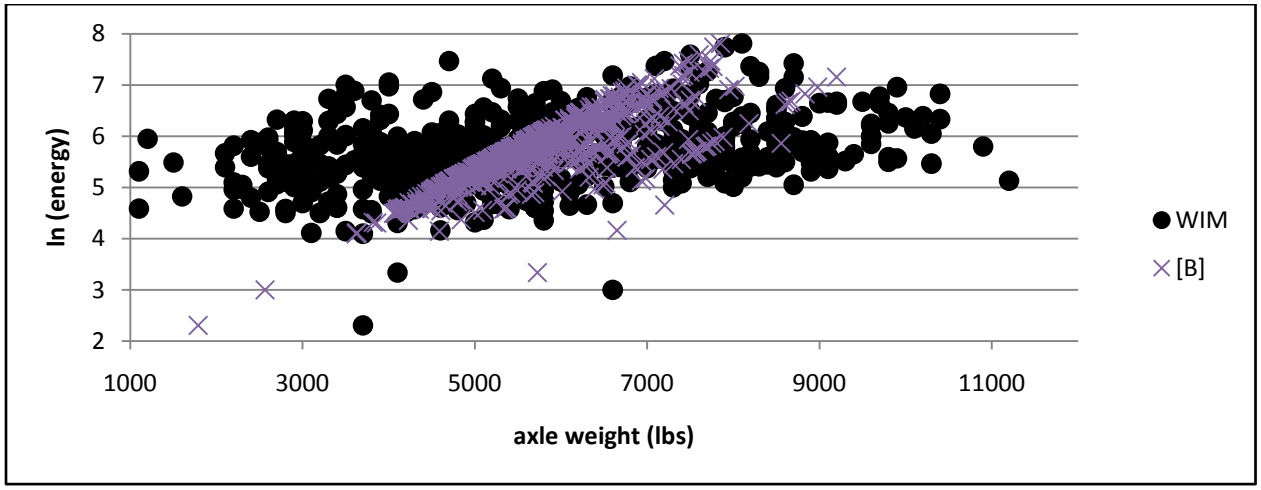

Figure 36 Model B - axle weight as a function of ln(energy)

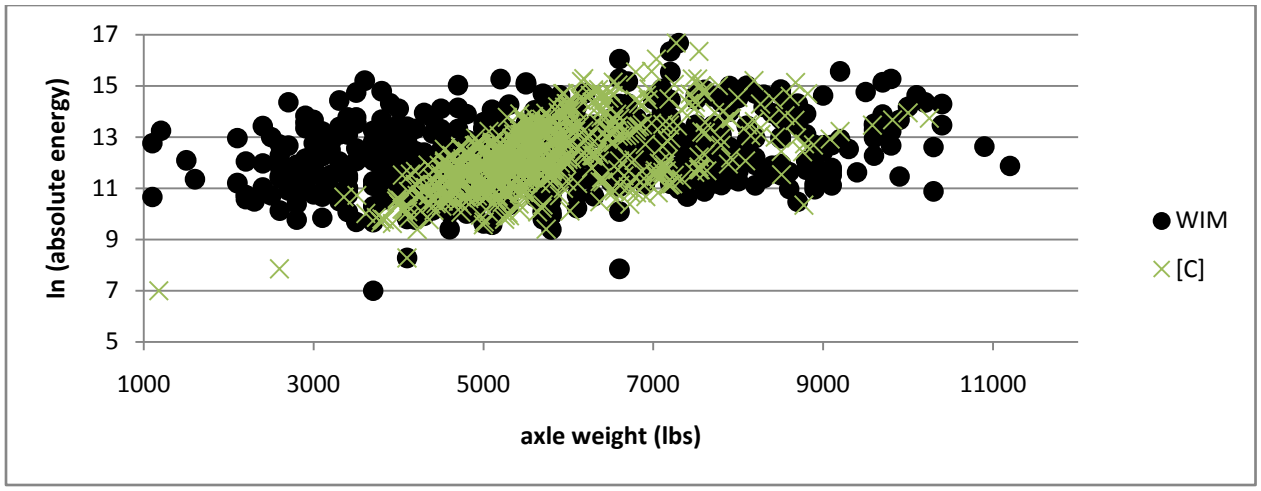

Figure 37 Model C - axle weight as a function of ln(absolute energy)

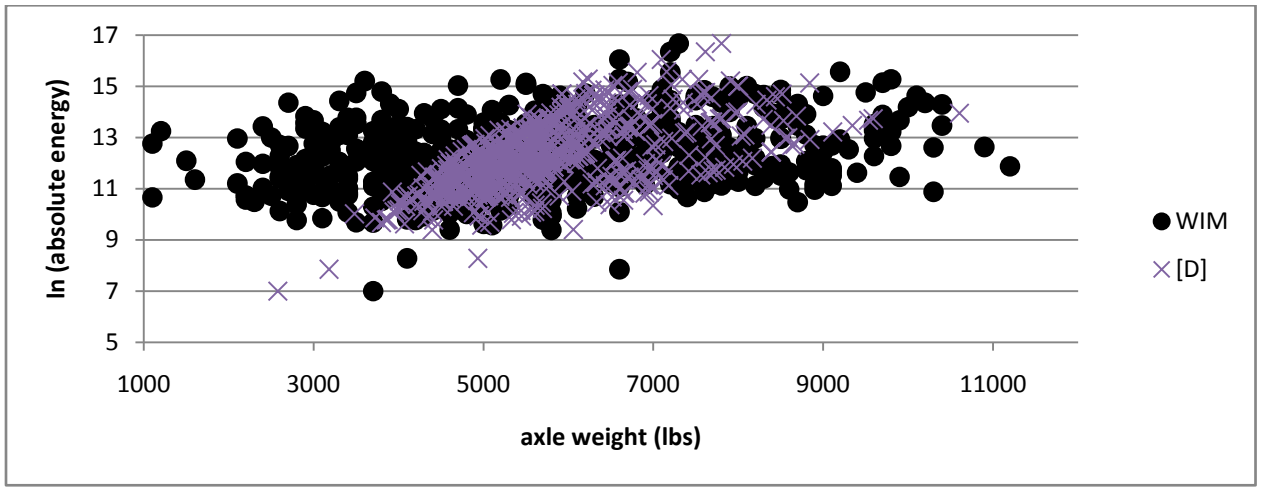

Figure 38 Model D – axle weight as a function of ln(absolute energy)

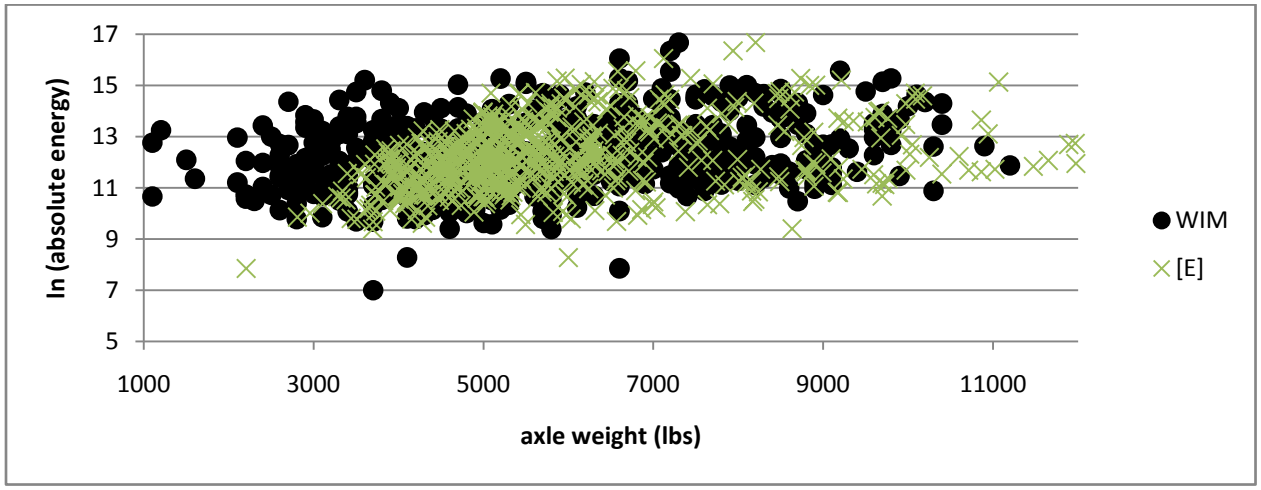

Figure 39 Model E – axle weight as a function of ln(absolute energy)

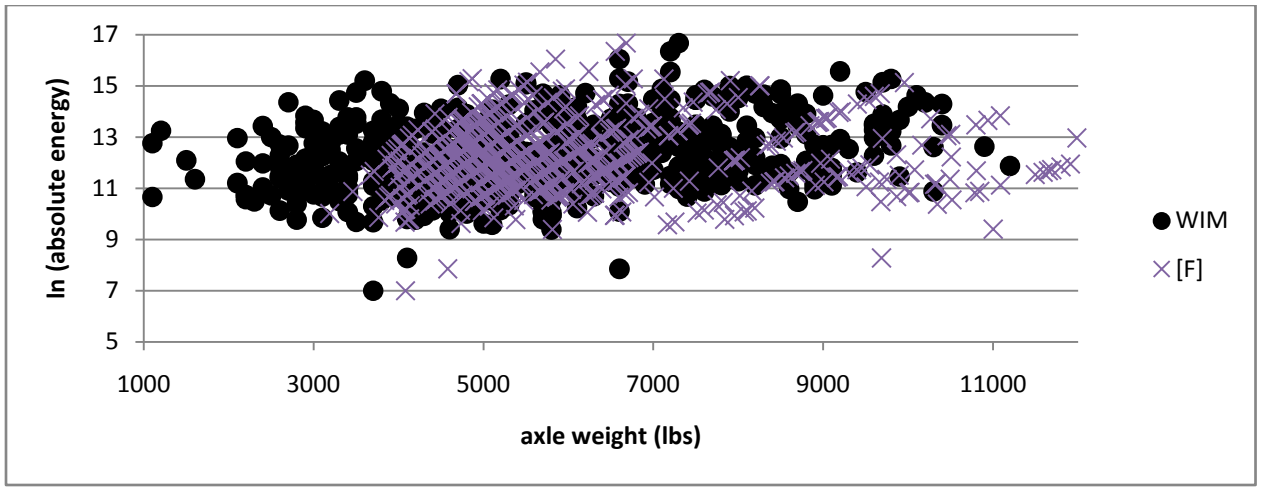

Figure 40 Model F – axle weight as a function of ln(absolute energy)

When the HAWs for each vehicle are added together so that predicted gross vehicle weights can be compared to actual gross vehicle weights, the efficacy of the models is more apparent. Figure 41 through Figure 43 show the predicted gross vehicle weights compared to actual gross vehicle weights for the models. In addition, Table 9 shows the results of paired t-tests comparing the results from each model with the actual values. A histogram of the residuals is shown in Figure 44, for comparison with the results in Experiment D. Models B, C, and D are shown to be the most accurate models.

It should be noted that it was not possible to record the exact horizontal location at which the truck tire struck the metal test strip; however, this value did not vary greatly from one truck to another. The WIM has an off-center sensor that detects trucks that are not travelling down the center of the lane, so most trucks follow the same path.

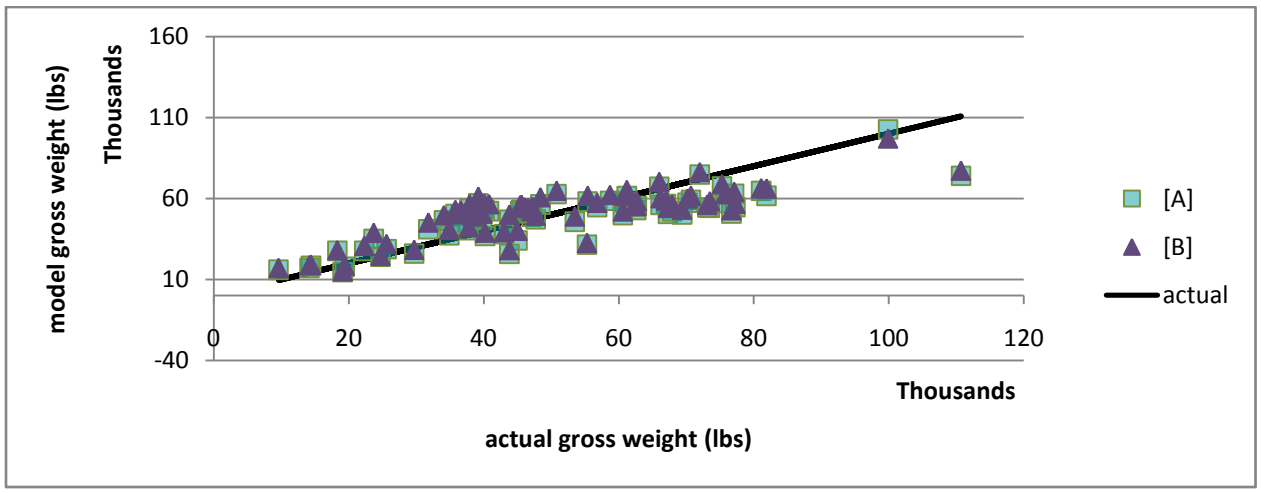

Figure 41 Models A and B – gross vehicle weight comparison

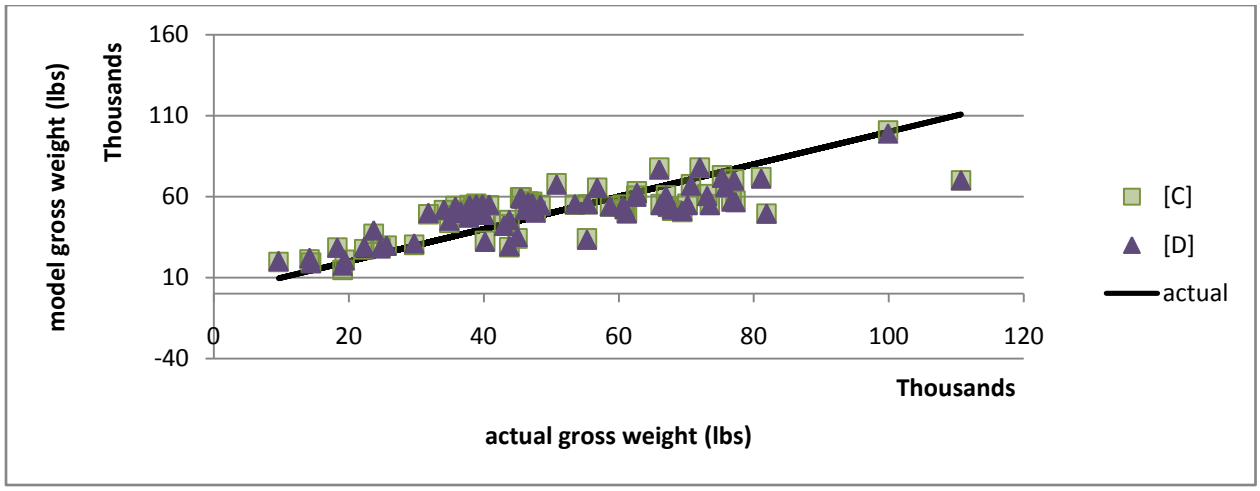

Figure 42 Models C and D – gross vehicle weight comparison

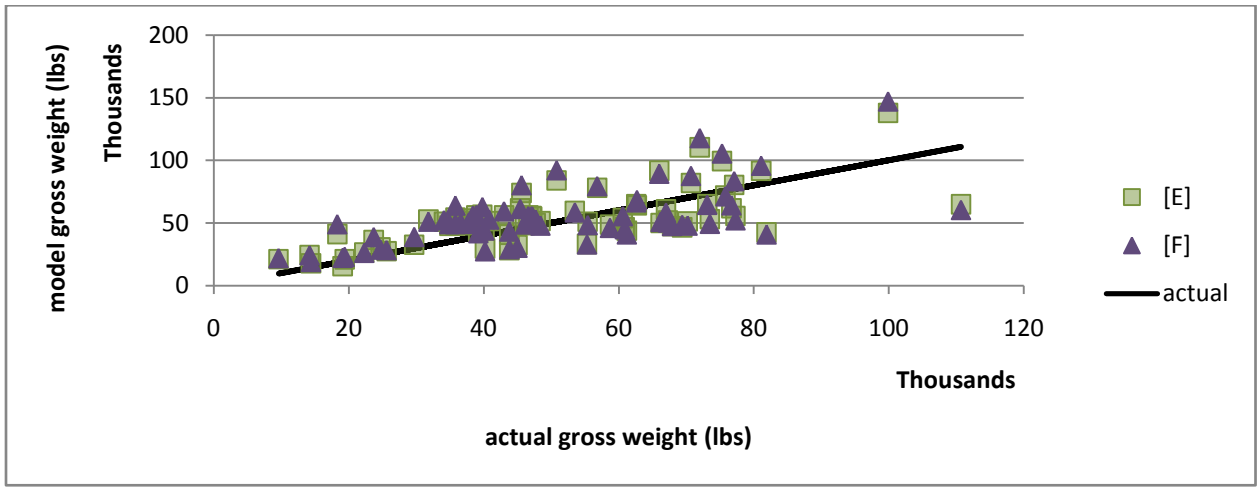

Figure 43 Models E and F – gross vehicle weight comparison

Table 9 P-values from paired t-tests comparing model results to actual weights

Model	Half axle weight (HAW)	Gross vehicle weight
A	0.0003	0.12
B	0.45	0.75
C	0.45	0.74
D	0.53	0.79
E	0.0004	0.15
F	0.00003	0.08

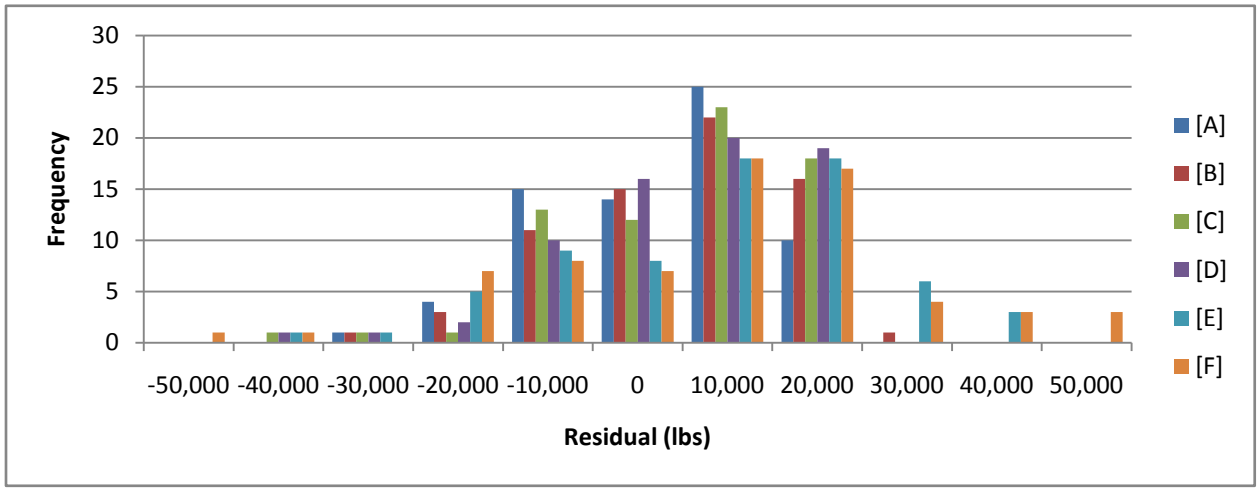

Figure 44 Gross vehicle weight residuals for models A through F, Experiment F

5 Discussion

The development of a low-cost WIM system using acoustic waves transmitted through a metal strip when struck by a moving vehicle shows promise; however, more research is needed to improve upon the methodologies and equipment used in these experiments before a working low-cost WIM system can be built. Six experiments were performed with the intent of relating acoustic emission parameters to load (weight or speed of a moving vehicle). Table 10 shows the acoustic emission parameters that were shown to be correlated with load or speed in each of the six experiments.

Table 10 Parameters correlating acoustic emission and weight of a moving vehicle

	Parameter associated with load	Parameter associated with speed
A	• absolute energy	
B		• maximum wavelet coefficient
C	• maximum count, energy, absolute energy	
D	• location, • sum of absolute energy, counts to peak • maximum energy, count, duration, counts to peak	
E		• acoustic emission duration
F	• speed, • maximum counts to peak, energy, absolute energy, rise time, duration, count	

5.1 Parameters associated with speed

Because the speed of the vehicle affects acoustic emission response values, the parameters shown to be associated with speed (wavelet coefficient and acoustic emission duration) might be

helpful in determining the weight of a vehicle based on the acoustic emission response. Unfortunately, neither of these values can currently be used to improve a regression analysis relating load and the acoustic emission parameters. The difficulty with the wavelet coefficient is merely a convenience problem – additional software beyond the AEWin software must be used to determine the wavelet coefficient, and the data then must be manually entered. In order to use the wavelet coefficient effectively, this process would need to be streamlined. The difficulty with the acoustic emission duration, however, is more enduring. When the vehicles are moving at highway speeds, there is not time for the acoustic vibrations to have died away between ABs; therefore, acoustic emission duration cannot be determined.

5.2 Parameters associated with load

Many parameters were shown to be helpful in predicting load from acoustic emission response.

5.2.1 Location (distance of TB from sensor)

Experiment D showed clearly that the acoustic emission values were higher when the TB occurred closer to the sensor. Figure 45 summarizes the data shown in Figure 24, showing how much the acoustic emission energy changes with distance of the event from the sensor. Unfortunately, the location of the TB could not be measured during Experiment F. Depending on how sensitive the acoustic emission values are to location, including a measurement of location in future experiments might help to create a more accurate model.

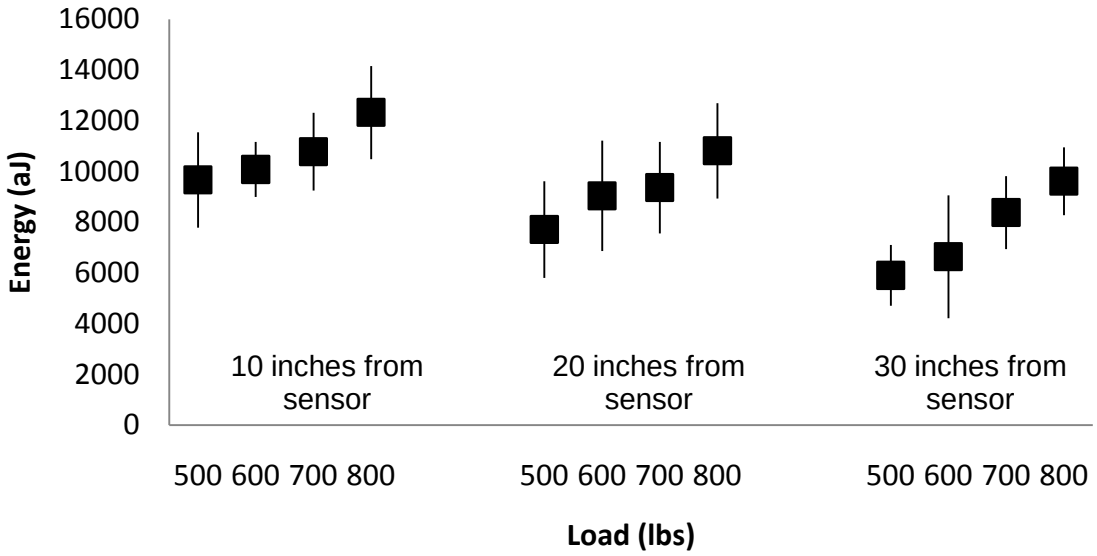

Figure 45 Energy as a function of load, by location

5.2.2 Speed

Vehicles traveling at high speeds create higher acoustic emission responses than vehicles of the same weight traveling at lower speeds. This makes sense, because the WIM system we are proposing measures the kinetic weight of the vehicle, not the static weight. In Experiment F, speed was an important part of the regression model in every case. In addition, it appears that the

relationship of speed and acoustic parameters to load is not simply linear, as it was helpful to include a quadratic term for speed in the regression models.

5.2.3 Energy and absolute energy

That the energy and absolute energy of the acoustic emission response would be related to the load of the moving vehicle is intuitively obvious. Indeed, energy and/or absolute energy was shown repeatedly to be related to load. Since energy and absolute energy are linearly related to each other, both parameters were not included in every model, but every regression model contained at least one of these parameters.

5.2.4 Count, counts to peak, rise time, and duration

Count, count to peak, rise time, and duration were also useful in models for load. In Experiment C, count was the only one of these parameters where a clear relationship between count and load could be seen graphically. Nevertheless, all of these parameters were useful in at least one of the regression models developed in the analysis of Experiment F.

5.3 Determination of location of event

The determination of the horizontal location at which the tire or axle struck the metal test strip was not a primary focus of this research, but it was examined briefly. Although the AEWin software was able to determine the location of a simple event such as a lead break, the software was not very successful with complicated events such as a TB. If this topic were to be pursued in the future, it would be necessary to create a more sophisticated algorithm for determining the horizontal location of a TB or AB.

5.4 Low-cost WIM equipment

The equipment used in the experiments presented here was generally of high quality and suitable for this application; however, future experiments of this type should consider the following modifications:

- Portable PCI card system. The PCI card that was used in the field was susceptible to heat. In addition, the card must be used in a desktop computer, making it difficult to use in the field. The same functionality is available using a PCI card in a portable, battery powered case that can connect directly to a laptop computer.
- Better machining of metal test strip. A groove was machined along the bottom side of the metal test strip used in Experiment F. Because of the difficulty in machining a groove from a bar of this length (approximately 75 inches), the groove is not completely smooth, which may have contributed to the variability of the acoustic emission response. The groove is valuable because it protects the sensors and their cables from the heavy vehicles. Methods should be sought to obtain these benefits without risking breakage of the test strip and without introducing variability.

6 Conclusion

This paper reports on a series of six experiments performed as part of FDOT Contract 16507036 to develop a low-cost system for weighing heavy vehicles at highway speed. The system included a metal strip instrumented with acoustic emission sensors to detect acoustic waves within the metal material. The researchers found that epoxy was a suitable material for affixing the metal strip to a road surface. The acoustic waves created in the metal strip when a vehicle rolled over the strip were digitized via the acoustic emission sensors and the acoustic emission response was collected by a computer.

The researchers were able to find correlations between the weight of the vehicle crossing the metal strip and the acoustic response recorded by the computer. The energy and absolute energy of the acoustic emission response were found to be particularly important for predicting the vehicle weight. In addition, it was necessary to know the speed of the vehicle and the location along the metal strip where the vehicle's tires strike the strip in order to predict the vehicle weight.

The variability of the acoustic emission response was shown to be fairly high, resulting in imprecise values for predicted vehicle weight. Future research to examine this technology further should consider ways to reduce the variability of the acoustic emission response, including by improving the software and hardware used by the sensors and by machining a more uniform test strip.

7 References

Andrle, S., McCall, B., & Kroeger, D. (2002). *Application of Weigh-in-Motion (WIM) Technologies in Overweight Vehicle Enforcement.* Paper presented at the Third International Conference on Weigh-in-Motion, Orlando, Florida, USA.

Barros, R. T. (1985). Analysis of Pavement Damage Attributable to Overweight Trucks in New Jersey. In *Transportation Research Record: Journal of the Transportation Research Board* (Vol. 1038, pp. 1-9). Washington, D.C.: Transportation Research Board of the National Academies.

Bowie, J. M., Moslehy, F. A., & Oloufa, A. (2008). Development of a Low-Cost Weigh-in-Motion System. *Journal of Management & Engineering Integration (JMEI)*.

Chang, W., Sverdlova, N., Sonmez, U., & Strit, D. (2000). Vehicle Based Weigh-in-Motion System. *Heavy Veh Syst, 7*(2-3), 205-218.

Cole, D. J., & Cebon, D. (1989). *A capacitative strip sensor for measuring dynamic tyre forces*. Paper presented at the Second International Conference on Road Traffic Monitoring.

Collap, A. C., Al Hakim, B., & Thom, N. H. (2002). Effects of Weigh-in-Motion Errors on Pavement Thickness Design. *I MechE, 216 Part D*, 141-151.

Cunagin, W. D., Majdi, S. O., & Yeom, H. Y. (1991). Intelligent Weigh-in-Motion Systems. In *Transportation Research Record: Journal of the Transportation Research Board* (Vol. 1131, pp. 88-91). Washington, D.C.: Transportation Research Board of the National Academies.

Cunagin, W. D., Mickler, W. A., & Wright, C. (1997). Evasion of Weight-Enforcement Stations by Trucks. In *Transportation Research Record: Journal of the Transportation Research Board* (Vol. 1570, pp. 181-190). Washington, D.C.: Transportation Research Board of the National Academies.

Davies, P., & Sommerville, F. (1987). Calibration and Accuracy Testing of Weigh-in-Motion Systems. In *Transportation Research Record: Journal of the Transportation Research Board* (Vol. 1123, pp. 122-126). Washington, D.C.: Transportation Research Board of the National Academies.

Gagarine, N., Flood, I., & Albrecht, P. (1992). *Weighing Trucks in Motion Using Gaussian-Based Neural Networks*. Paper presented at the International Joint Conference on Neural Networks.

Hajek, J. J., Kennepohl, G., & Billing, J. R. (1992). Applications of Weigh-in-Motion Data in Transportation Planning. In *Transportation Research Record: Journal of the Transportation Research Board* (Vol. 1364, pp. 169-178). Washington, D.C.: Transportation Research Board of the National Academies.

Izadmehr, B., & Lee, C. E. (1987). On-Site Calibration of Weigh-in-Motion Systems. In *Transportation Research Record: Journal of the Transportation Research Board* (Vol. 1123, pp. 136-144). Washington, D.C.: Transportation Research Board of the National Academies.

Mimbela, L.-E. Y., Pate, J., Copeland, S., Kent, P. M., & Hamrick, J. (2003). *Applications of Fiber Optic Sensors in Weigh-in-Motion (WIM) Systems for Monitoring Truck Weights on Pavements and Structures* (No. SPR-3(185))o. Document Number)

Moslehy, F. A., & Oloufa, A. (2004). *Laser-Based Vibration Technique for Weight Measurement of Commercial Vehicles.* Paper presented at the IMAC XXII Conference on Structural Dynamics, Dearborn, MI.

Moslehy, F. A., Oloufa, A., & Bowie, J. M. (2007). *An Elegant Design of Weigh in Motion Test Apparatus.* Paper presented at the 2007 International Conference on Industry, Engineering, and Management Systems, Cocoa Beach, FL.

Papagiannakis, A. (1997). Calibration of Weigh-in-Motion Systems Through Dynamic Vehicle Simulation. *J. Test Eval, 25*(2), 197-204.

Sebaaly, P. E., Chizewick, T., Wass, G., & Cunagin, W. D. (1991). Methodology for Processing, Analyzing, and Storing Truck Weigh-in-Motion Data. In *Transportation Research Record: Journal of the Transportation Research Board* (Vol. 1311, pp. 51-59). Washington, D.C.: Transportation Research Board of the National Academies.

Stergioulas, L., Cebon, D., & Macleod, M. (2000). Static Weight Estimation and System Design for Multiple-Sensor Weigh-in-Motion. *I MechE, 214 Part C*, 1019-1035.

Truck Weight Limits: Issues and Options, Special Report 225. (1990). Washington, D.C.: Transportation Research Board of the National Academies.

U.S. Department of Transportation. (2006). *Freight in America: A New National Picture*. Washington, D.C.: Research and Innovative Technology Administration/Bureau of Transportation Statistics.

APPENDIX

Stress Analysis of Metal Test Strip

STEEL RUMBLE STRIP ANALYSIS

The Model Dimensions:

- Section as given by the Autocad drawing
- Length 12" (a portion of the strip)

Material Properties:

- E=29E6 psi
- υ=0.3

Boundary Conditions

- The bar is attached to the ground by epoxy glue. Assuming that the glue hold as expected, the bottom nodes are restrained against movement in three directions.

The Loading Assumptions:

-Tire width is 8.5" (which seems to be the least width)

-Load is 11,000 lbs which is uniformly distributed over the tire print. Tire print width is kept too narrow to concentrate the loading in the middle to get the highest stress effects.

-Loading is right at the top nodes (presumably the worst case scenario)

-Load is centered along the length (see Figure 3)

Figure 1. The FE mesh of the cross section

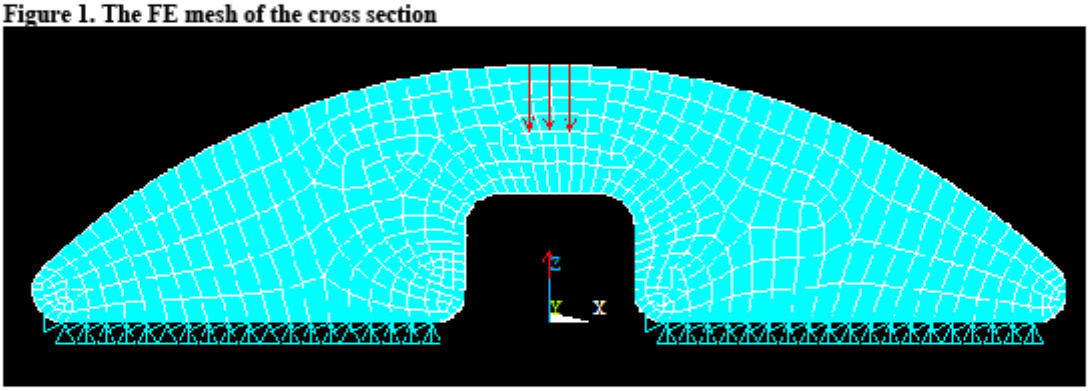

Figure 2. Perspective view of the FE mesh

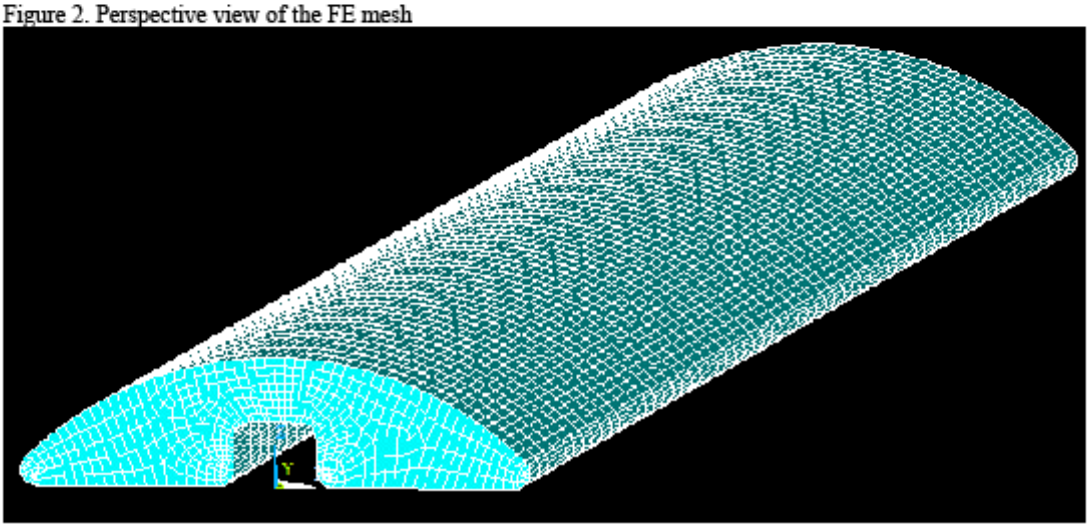

Figure 3. The top view of the loaded nodes

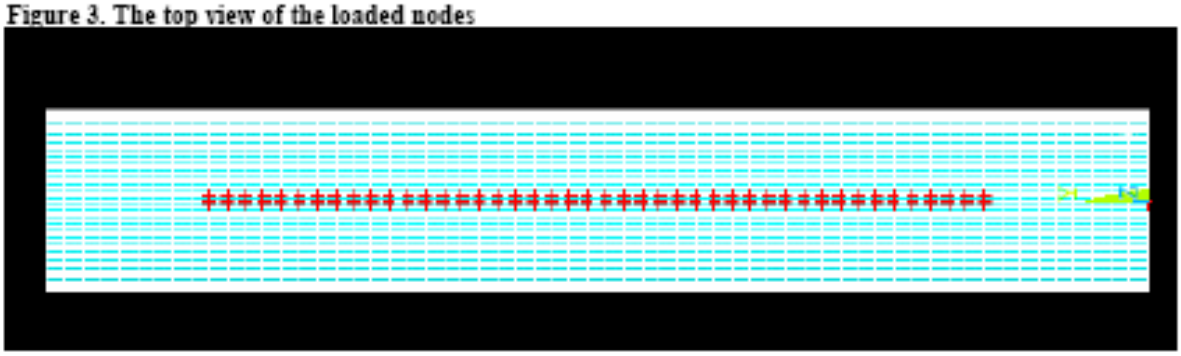

Figure 4. Vertical displacement contours UzMax=0.109e-3 inches (downward)

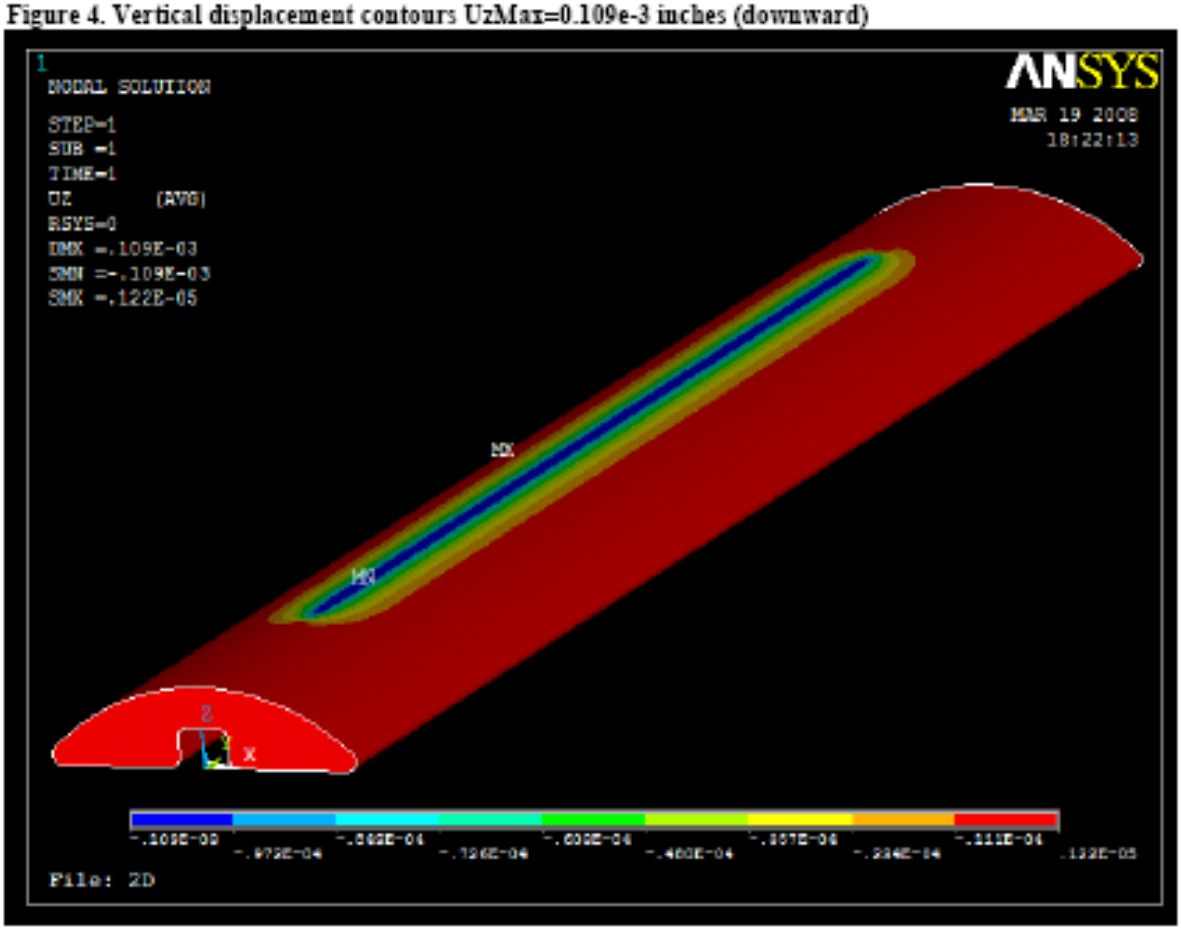

Figure 5. Bending stress Sx contours: SxMax=5,072 psi (tension), SxMin=13,682 psi (compression)

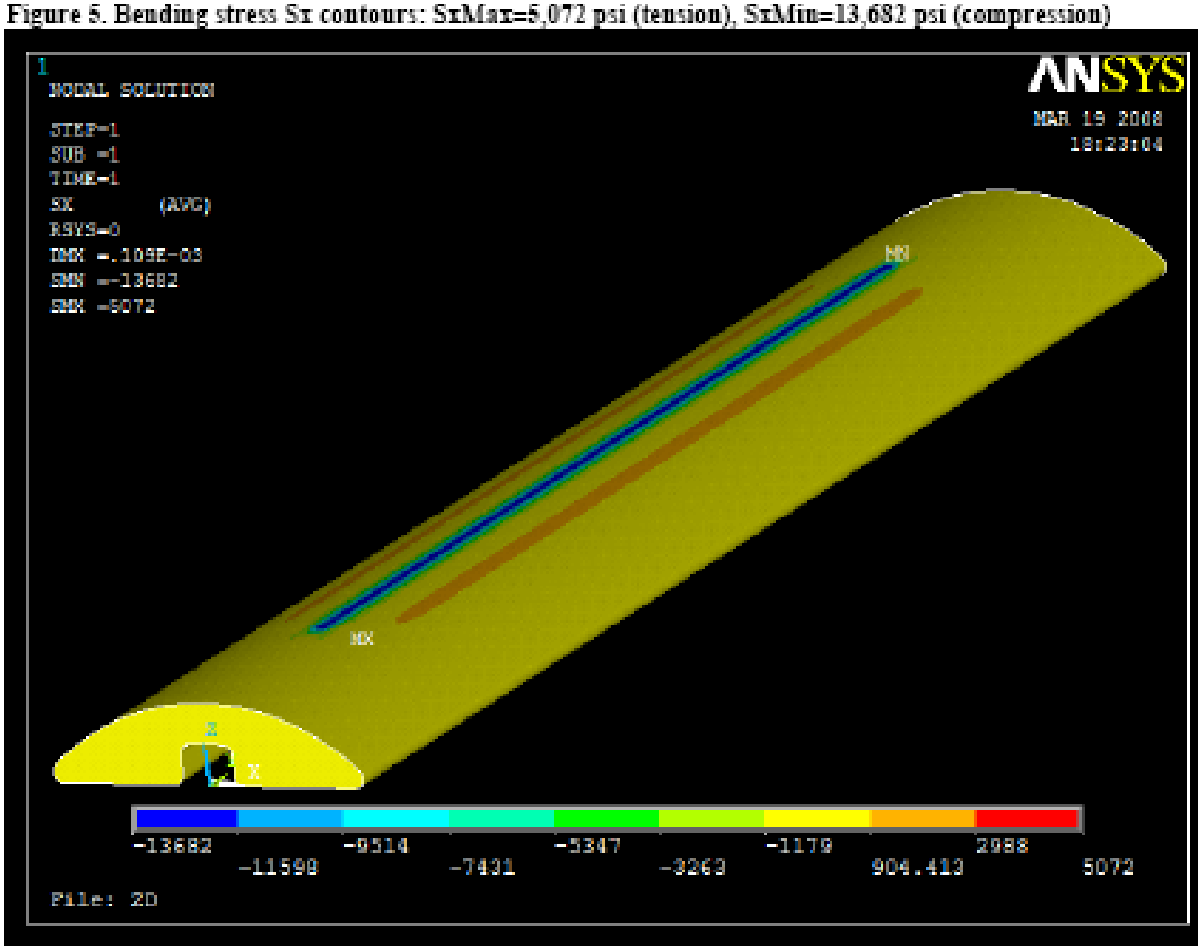

Figure 6. VonMises stress contours: SMax=9,557 psi

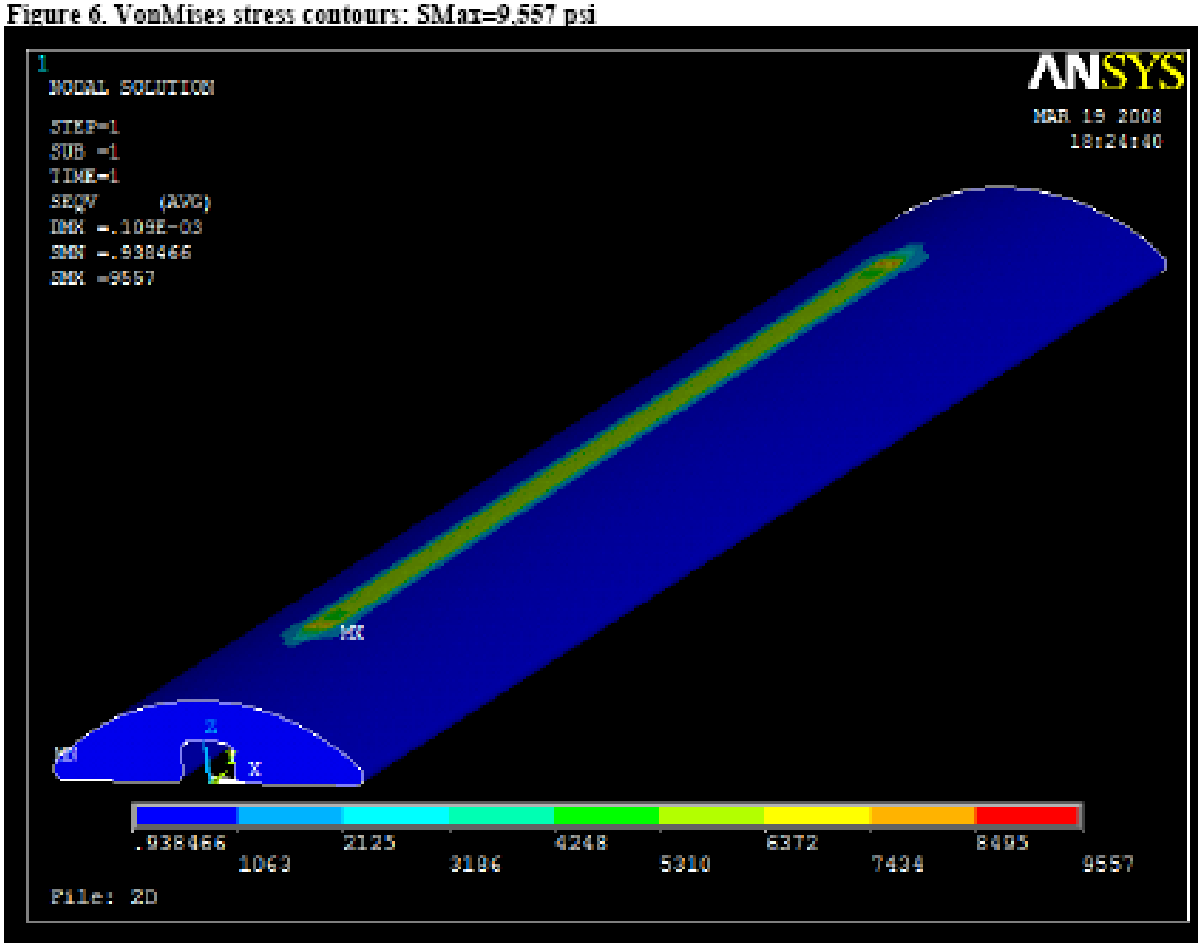

Figure 7. Vertical displacement contours at the middle cross section. UzMax=0.109e-3 inches (downward)

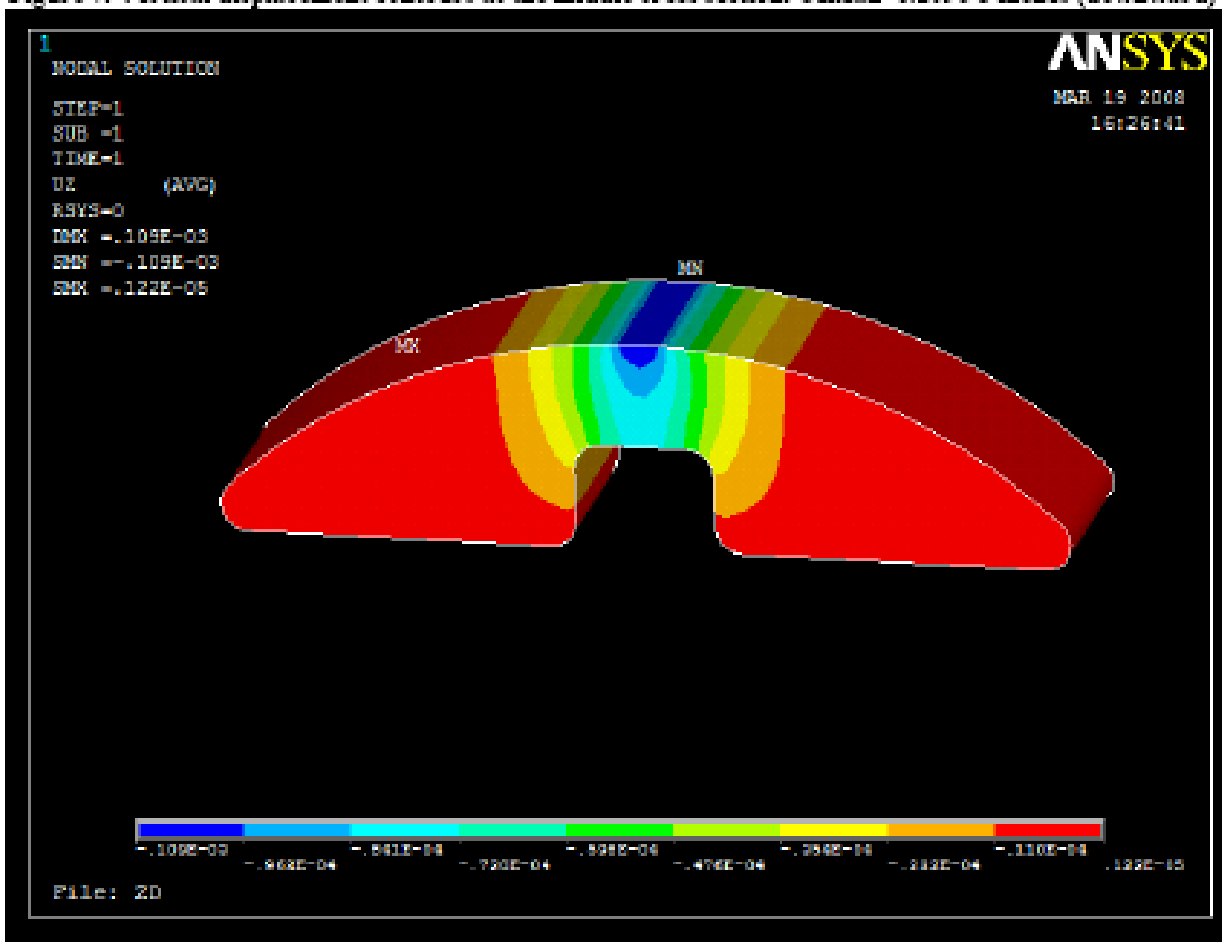

Figure 8. Bending stress Sx contours: SxMax=5,030 psi (tension), SxMin=13,268 psi (compression)

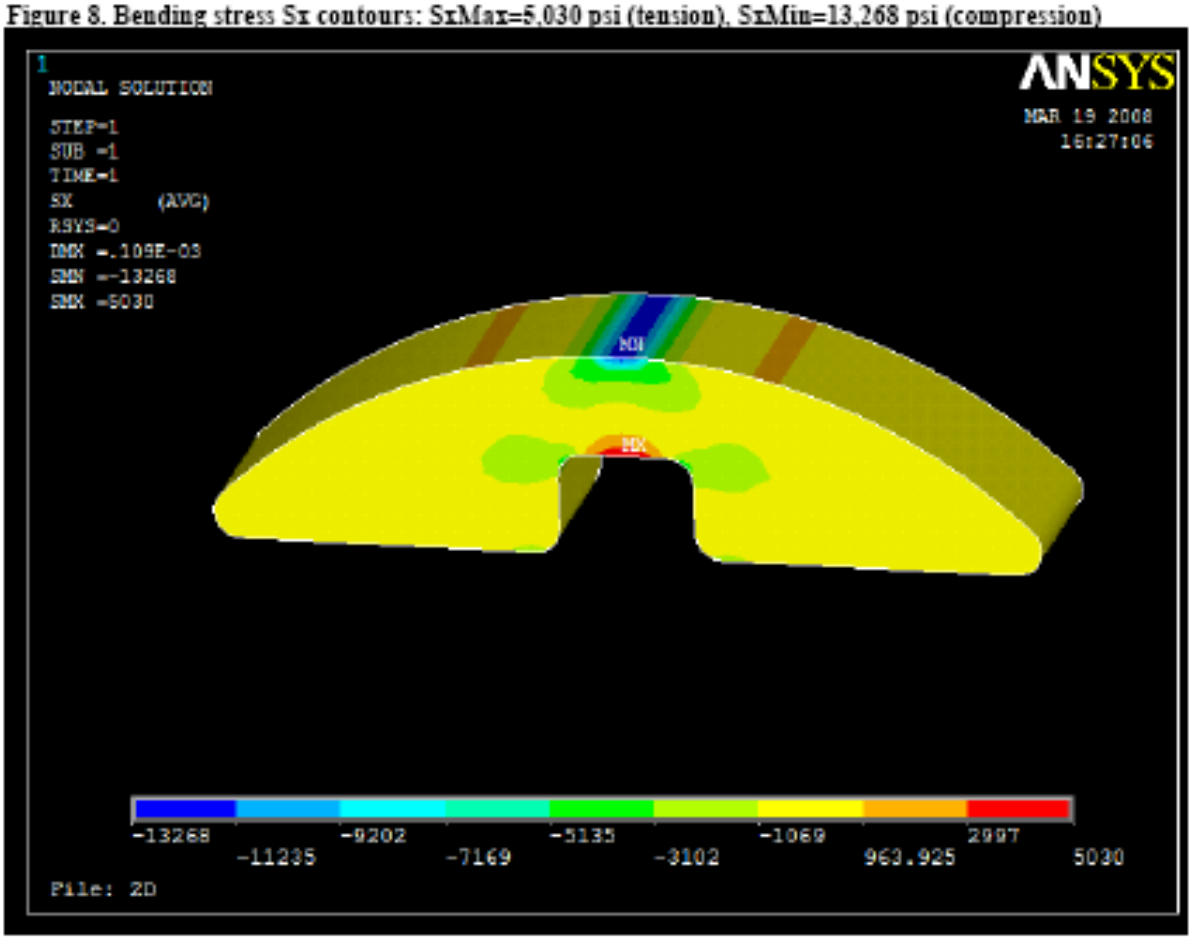

Figure 9. VonMises stress contours at the middle cross section: SMax=9.473 psi

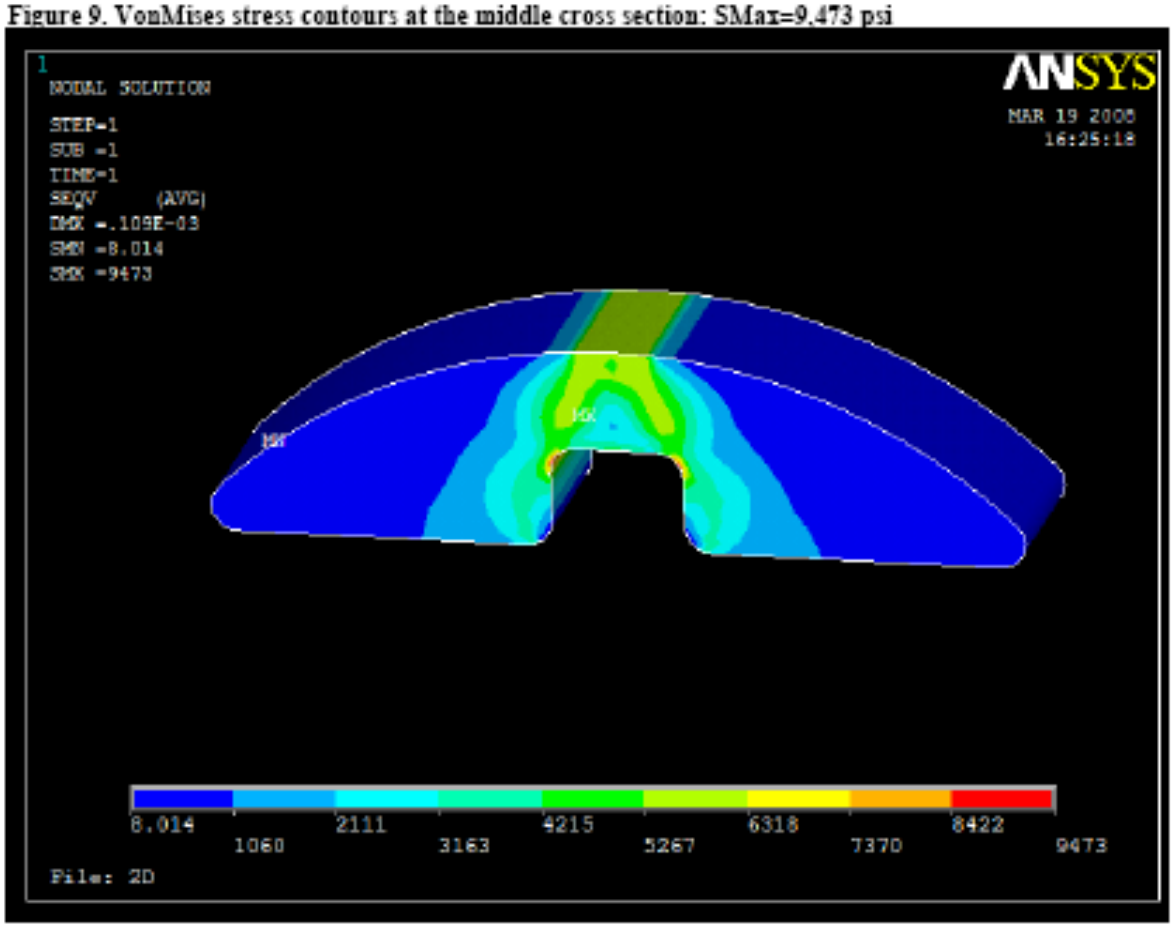

You may want to find out the yielding stress of the steel bar you have. (It is probably A36 steel which has a yielding stress of 36,000 psi.)